Available online at www.sciencedirect.com
SCIENCE DIRECT®
Journal of Sound and Vibration 275 (2004) 795–822
JOURNAL OF SOUND AND VIBRATION
www.elsevier.com/locate/jsvi

# Dynamics of an oblique-impact vibrating system of two degrees of freedom

W. Han[a,b], D.P. Jin[a], H.Y. Hu[a,*]

[a] *Institute of Vibration Engineering Research, Nanjing University of Aeronautics and Astronautics, 210016 Nanjing, People's Republic of China*

[b] *Department of Mechanical Engineering, Naval Aeronautical Engineering Academy, 264001 Yantai, People's Republic of China*

Received 5 November 2002; accepted 26 June 2003

**Abstract**

The dynamic analysis of oblique-impact vibration is presented in this paper through an illustrative system, where a spring–pendulum obliquely collides a mass–spring oscillator. The oblique-impact process and the relations between the pre-impact state and the post-impact state of system are analyzed first upon a hypothesis on instantaneous oblique impacts. On the basis of the oblique-impact relations, then, the dynamic equation of such an oblique-impact vibrating system is established. Consequently, the existence and the stability of the periodic motions are analyzed and a series of analytical solutions are derived in some simplified cases. Afterwards, the transitions of the steady state motions of the system with the variation of the excitation, the damping and the contact–friction are numerically studied in general cases. The study shows that the coefficient of restitution for an oblique-impact cannot be regarded as a constant, and that the relations between the pre-impact state and the post-impact state are directly associated with the impact angle and the coefficient of contact–friction between impacting bodies. For the system of concern, the system parameters and initial states have to be carefully selected if any stable periodic motion is expected. Furthermore, very rich dynamic behaviors, such as bifurcations and chaotic motions, are observed in the numerical results.


## 1. Introduction

The mechanical system with a clearance between two moving parts is quite popular in engineering. Vibro-impacts occur when the moving parts repeatedly collide with each other so

*Corresponding author. Tel.: +86-25-4893278; fax: +86-25-4891512.
*E-mail address:* hhyae@nuaa.edu.cn (H.Y. Hu).

0022-460X/$ - see front matter © 2003 Elsevier Ltd. All rights reserved.
doi:10.1016/S0022-460X(03)00743-0

that the system exhibits very complex non-linear dynamics [1,2]. Great attention has been paid to the vibro-impact problems over the past decades because of their significance on the performance and life of mechanical systems. However, it is far from an easy task to solve the vibro-impact problems with strong non-linearity and non-smoothness.

In most vibro-impact problems, the impact duration is very short compared with the period of vibration of concern. For instance, it takes only $10^{-5}$–$10^{-3}$ s for a normal impact between two bodies made of metals. Hence, some essential assumptions have been introduced in the widely used model, like, Newton's quasi-rigid bodies impact model [3] as following. (1) The impact duration $\Delta t$ is assumed to be infinitesimal and the impact force $\mathbf{F}$ to be infinitely large so that the impact impulse and the changes of impact velocity are finite values. (2) All forces except the impact force are finite and can be ignored during the impact. (3) The deformations of impacting bodies keep within a tiny region. (4) The contact surface between the impacting bodies is smooth, and then the friction can be ignored. As a result, a coefficient of restitution $r \in [0, 1]$ can be introduced to describe the relation between the pre-impact state and the post-impact state, and the energy dissipation during the impact such that no details during the impact should be analyzed. For example, the relation of relative velocity of two impacting bodies can be expressed as

$$\mathbf{v}_f \cdot \mathbf{n} = -r\,\mathbf{v}_0 \cdot \mathbf{n}, \tag{1}$$

where $\mathbf{v}_0$ and $\mathbf{v}_f$ are the relative velocities of pre-impact and post-impact respectively and $\mathbf{n}$ denotes the normal direction of the impact surface. Because the friction between impacting bodies is not taken into account, such a model is usually used to describe the direct central impact when the relative velocity is along the normal direction or the direct eccentric impact without friction. These cases are hereinafter called the direct vibro-impact, which is distinguished from the oblique-impact vibration in any case when the friction is taken into consideration.

The direct vibro-impact model, or the Newton's impact law, was widely implemented to study the vibro-impact dynamics. Abundant results were observed in the theoretical, numerical and experiential studies on the vibro-impacting systems of single degrees of freedom [1,4–9]. Especially, Foale and Bishop [7], Hu [8,9] respectively studied the grazing bifurcation in a vibro-impact system and indicated that the grazing bifurcation can suddenly change the stability of periodic motions and then give rise to chaotic motions. In the studies on the vibro-impacting systems of multiple degrees of freedom, Bishop et al. [10] predicted the period-1 impacts in a driven beam by virtue of the rigid-body impact model and examined the results in an experiment. Ivanov [11] proposed a unified approach to the analysis of vibro-impact, of which the mathematical essence was the continuous representation of the impulsive motion in some auxiliary variables, and then investigated the stability and the bifurcation by using the Floquet theory and studied the grazing bifurcation by taking the finite impact duration into account. Toulemonde and Gontier [12,13] studied a vibro-impact system of multiple degrees of freedom based on a predictor–corrector method, and found the complex phenomena such as flip bifurcation, saddle-node bifurcation, Hopf bifurcation and grazing bifurcation, and the stick–slip, which may lead to non-zero impact duration. Luo and Xie et al. [14,15] investigated a type of vibro-impacting systems of two degrees of freedom in detail by virtue of the mapping method. Recently, Kember and Babitsky [16] used the periodic Green function method to continuously compute the integral of the vibro-impacting system of two degrees of freedom. Jin and Hu [17], Li and Lu [18] respectively investigated the periodic motions of a type of vibro-impacting systems

of dual components, and determined the analytical solution of period-$n-1$ motions and their stabilities. In most cases, however, the studies focused on the qualitative or numerical analysis because of the complexity of any non-linear dynamic systems of multiple degrees of freedom.

In contrast with the direct-impact, the oblique-impact is more complex. During an oblique-impact process, there exists not only the normal relative velocity, but also the tangential relative velocity of the impacting bodies on the contact regions. The former results in the normal deformation, whereas the latter gives rise to the tangential deformation if there is any friction on the contact regions. Babitsky studied the oblique impact by virtue of the Newton's impact law and the Coulomb's law of friction in his monograph [19]. In the study on the oblique impact problem of single degree of freedom, Lv [20], Ratner and Styller [21] named the friction during impact as "instantaneous friction" or "dynamic friction", which were distinguished from the static friction and the sliding friction in general cases. Lv [3] defined the "coefficient of instantaneous friction" $\mu$ satisfying

$$P_t \leqslant \mu P_n, \tag{2}$$

where $P_n$ and $P_t$ are the normal impact impulse and the tangential impact impulse, respectively. Then, he introduced the "coefficient of tangential restitution" $r_\tau$ satisfying

$$v_\tau^+ = r_\tau v_\tau^-, \tag{3}$$

where $v_\tau^-$ and $v_\tau^+$ are the tangential relative velocity of pre-impact and post-impact, respectively. In Ref. [20], the measured values of "$r_\tau$" were given for a few types of materials. Furthermore, Ratner and Styller [21] found the relation among the coefficient of friction $\mu$, the impact velocity and the impact angle:

$$\mu = (v_0 \cos\alpha_0 - v_f \cos\alpha_f)/(v_0 \sin\alpha_0 + v_f \sin\alpha_f), \tag{4}$$

where $v_0$, $\alpha_0$, $v_f$ and $\alpha_f$ are the absolute velocity and the attack angle of the velocity of pre-impact and post-impact, respectively.

The above ideas and results are reasonable, but applicable to a few special cases only. For example, Eq. (4) only holds in the case of an oblique-impact between a free body and an elastic plane. On the other hand, the definition and the measurement of the "coefficient of instantaneous friction" are very difficult and even quite arbitrary. Furthermore, $r_\tau$ and $\mu$ are interdependent and are associated with the impact velocity and angle. So, these results have not yet been generalized to the other cases of oblique-impact.

Brach [22] illustrated that the tiny slip might stop during an oblique-impact owing to friction and then either the direction of slip reversed or the contact points rolled without slip during an oblique-impact process involving friction. The impact complexity may give rise to an erroneous increase in energy by virtue of the theory based on Newton's impact law in some special cases. To resolve the above paradox, Stronge [23,24] studied the energy dissipation and proposed a new definition where the coefficient of restitution $e$ was independent of friction. In his result, $e$ defined on the basis of energy dissipation is uniquely valid. As an example, $e$ was deduced in the case of the oblique-impact between a pendulum and the fixed rigid plane. Furthermore, the viewpoint was generalized to the three-dimensional impact [25].

Wang and Mason [26] used Routh's graphical method to describe an oblique-impact process of two rigid-bodies and to determine the frictional impulse. Lewis and Rogers [27] observed in an

experiment that the transitions in both normal and tangential forces were synchronous if a single direction micro-slip exists in the oblique-impact process. This evidence means that the tangential force and the normal impact force reach their maximal values simultaneously. Furthermore, the asynchronous phenomena of the transitions in normal and tangential forces were reported in other cases [28,29].

In summary, the studies on oblique-impacts are less intensive than those on direct-impacts. Most studies are confined to some special case studies and are not applicable to the general problems of oblique-impacts.

The work presented in this paper focuses on the dynamics of an oblique-impact vibrating system of two degrees of freedom, composed of a spring–pendulum and a mass–spring oscillator. The relation between the pre-impact state and the post-impact state will be deduced in Section 2. In Section 3, the dynamic equation of the oblique-impact vibrating system will be established, and then the existence and the stability of the periodic motions will be analyzed. In Section 4, numerical results will be given to show the transitions of the steady state motions of the system with the variation of excitation, damping and friction. Finally, some conclusions will be drawn in Section 5.

## 2. Analysis of oblique-impact process of a pendulum–oscillator system

A crucial issue in studying the dynamics of an oblique-impact vibrating system is to establish a simple, but reasonable impact model or a right computational method for the relation between the pre-impact state and the post-impact state. The impact model or the method, which links the pre-impact state and the post-impact state, is the basis of the study on oblique-impacts. This section, hence, focuses on the relations of the pre-impact state and the post-impact state for an oblique-impact.

The illustrative dynamic system of concern, placed on a horizontal plane, is composed of a spring–pendulum and a mass–spring oscillator as shown in Fig. 1. The spring–pendulum consists of a lumped tip mass $M_1$, a massless bar of length $l$, a flexible torsional component of linear stiffness $K_1$ and linear damping coefficient $C_1$. The volume of tip mass is negligible such that the

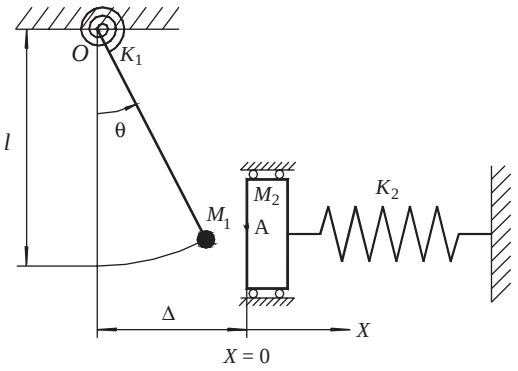


Fig. 1. An oblique-impact vibrating system of two degrees of freedom.

motion of pendulum is only the rotation about the fixed point $O$. The mass–spring oscillator includes a lumped mass $M_2$, a flexible component of linear stiffness $K_2$ and linear damping coefficient $C_2$. Furthermore, the pendulum and the oscillator are subject to the harmonic moment excitation of $f_{10}\cos(\Omega T+\varphi)$ and the harmonic force excitation of $f_{20}\cos(\Omega T+\varphi)$, respectively. The coefficient of friction between mass $M_1$ and the left surface of mass $M_2$ is $\mu$. In the process of vibration, mass $M_1$ will contact the left surface of mass $M_2$ at the position $A$ with an initial angle $\theta_0$ and initial angular velocity $\dot{\theta}_0$ at the moment $t_0$.

In the studies on the dynamics of the vibro-impact systems, the hypothesis of instantaneous impacts, which have been observed in various experiments of normal impacts, have been widely used. In this study, the hypothesis will be extended to the case of oblique-impact. That is, the oblique-impact occurs instantaneously like a normal impact, including micro normal compress and restitution deformation in the contact area during the impact process. So, the impact process can be divided into the approach phase and the restitution phase such that the laws of classical dynamics can be used in each phase. Furthermore, the complicated tangential motions such as the relative micro-slip in single direction or its trend, or the slip-reverse can be properly analyzed during an oblique-impact process, and the tangential friction in the contact surface can also be properly introduced. In a recent study [30], the hypothesis of instantaneous oblique impact has been confirmed through the detailed elastic-plastic analysis and an experiment for the case when the attack angle $\theta$ of impact is not very large and the initial relative normal velocity of two colliding bodies is not very low. In this case, the instantaneous impact or instantaneous slip-reverse does not result in any variation of macro-relative displacement. For the system in Fig. 1, the variation of angle $\theta$ arising from the micro-slip in the impact process is negligible and it is enough to use $(\dot{\theta},\dot{X})$ to characterize the state of system in the impact process. As a consequence, the relation between the pre-impact state and the post-impact state only includes the variation of relative velocity of two colliding bodies as in the case of normal impact.

For a normal impact, the coefficient of restitution, which plays an important role in the impact model of two quasi-rigid bodies, is often considered as a synthetical parameter related to the material behavior of impacting bodies and the environment conditions around the impacting regions. The coefficient of restitution was initially defined by Newton as a ratio between the relative velocities of post-impact and pre-impact, but the study on the impact mechanism was avoided. Like the coefficient of friction, there are hitherto some unclear problems in the mechanism study of the coefficient of restitution, especially in the case of impact with friction.

There are basically three ways to define the coefficient of restitution. For the impact between quasi-rigid bodies 1 and 2, with the positive direction of the common normal $\mathbf{n}$ of the contact surface defined from Body 1 to Body 2, the coefficient of restitution can be defined as follows:

(1) Newton's impact law is based on the variation of relative velocity of two impacting bodies and can be written as $r(\mathbf{v})=-(\Delta\mathbf{v}^{+}\cdot\mathbf{n})/(\Delta\mathbf{v}^{-}\cdot\mathbf{n})$, where $\Delta\mathbf{v}^{-}$ represents the relative velocity between two impacting bodies of pre-impact, and $\Delta\mathbf{v}^{+}$ represents the relative velocity between two impacting bodies of post-impact.

(2) Poisson's impact law is based on the variation of momentums of two impacting bodies and given by $r(\mathbf{P})=-(\mathbf{P}_{II}\cdot\mathbf{n})/(\mathbf{P}_{I}\cdot\mathbf{n})$, where $\mathbf{P}_{I}$ and $\mathbf{P}_{II}$ represent the momentums of two impacting bodies in the process of approach phase and restitution phase, respectively.

(3) Beghin–Boulanger impact law, or called Energy dissipation method, is based on the variation of the kinetic energy $\Delta W$ and given by $r(W) = \sqrt{|\Delta W_{II}/\Delta W_I|}$, where $\Delta W_I$ represents the variation of the kinetic energy of impact bodies in the process of approach phase, and $\Delta W_{II}$ represents the variation of the kinetic energy of impact bodies in the process of restitution phase, respectively.

Stronge [23,24], Wang and Mason [26] pointed out that the Beghin–Boulanger impact law includes the physical mechanism of impact because it relates to the non-elastic deformation of the impacting bodies. It has been already proved that the above three laws are equivalent in the case of direct-impact or in the case of oblique-impact without friction. If the approach phase and the restitution phase cannot be separated definitely, the third law is not effective and $r(\mathbf{v})$ does not equal $r(\mathbf{P})$ in the case of oblique-impact with friction. Like the coefficient of friction, the coefficient of restitution depends on the initial condition of impact and some other factors. The coefficient of restitution varies asymptotical from 1 to a constant less than 1 with an increase of normal impacting velocity from zero. In practice, the coefficient of restitution is often taken as a constant for simplicity.

When the hypothesis of instantaneous oblique impact is made and the tangential friction in the contact surfaces is taken into consideration, the switch of the approach phase and the restitution phase may be synchronous with the reverse of tangential micro-slip in a few cases. In general cases, the tangential motion falls into one of the following three cases, which include that the tangential micro-slip reverses within the normal approach phase or within the restitution phase in impact process, or it does not reverse in the impact process. Thus, the relation between the pre-impact state and the post-impact state cannot be described by using any simple impact laws, such as Newton's law or Poisson's law, especially in the case of an oblique-impact vibrating system of multiple degrees of freedom. To attack this problem, a numerical method, referred to as the incremental impulse method, was developed and experimentally verified in a recent study [30]. The method enables one to judge the direction of tangential micro-slip and to determine the state of the system at each incremental step of both normal impulse and tangential frictional impulse such that the possible reverse of tangential micro-slip due to friction can be properly determined. Compared with the analytical expressions applicable to a few of special vibro-impacting systems, the numerical method provides a widely feasible way for solving the oblique-impact problems of various dynamic systems.

In practice, it is almost impossible to establish any analytical relations between the pre-impact state and the post-impact state for most oblique-impact vibrating systems. However, one can fortunately find out the analytical relations for the above oblique-impact vibrating system in Fig. 1 according to whether the tangential friction is taken into account in the impact.

### 2.1. Oblique-impact relation with friction considered

A necessary condition for an impact between the pendulum and the oscillator is that the normal relative velocity of two sub-systems is positive when the corresponding normal relative displacement is getting to vanish. That is, $l\dot{\theta}_0 \cos\theta_0 - \dot{X}_0 > 0$ holds at the moment when an impact begins.

Now, two arbitrary moments, denoted by subscripts 1 and 2, during the impact process are considered. Then, $l\dot{\theta}_1 \cos\theta_0$, $\dot{X}_1$ and $l\dot{\theta}_2 \cos\theta_0$, $\dot{X}_2$ are the normal velocity of the pendulum and

the mass at these two moments, respectively. If $\dot{\theta}$ does not change its direction in the phase from moment 1 to moment 2, the impulse-moment principle gives

$$\dot{\theta}_2 = \dot{\theta}_1 - P[\cos\theta_0 + \mu\,\mathrm{sgn}(\dot{\theta}_1)\sin\theta_0],$$
$$\dot{x}_2 = \dot{x}_1 + \bar{m}P, \tag{5a, b}$$

where three dimensionless parameters $x = X/l$, $\bar{m} = M_1/M_2$ and $P = \bar{P}/(M_1 l)$ are defined, $\bar{P}$ is the normal impulse acting on the colliding bodies, and $\mu\bar{P}$ is the tangential impulse due to the Coulomb friction between the contact surfaces.

In the following analysis, the whole impact process will be divided into the normal approach phase, the possible phase when the tangential micro-slip reverses and the restitution phase. Thus, the termination conditions for different phases should be established. At the end of the normal approach phase, the terminal state of the system, denoted by $(\dot{\theta}_I, \dot{x}_I)$, satisfies

$$\dot{\theta}_I \cos\theta_0 - \dot{x}_I = 0. \tag{6}$$

At the reverse moment of tangential micro-slip, the angular velocity of the pendulum $\dot{\theta}_R$ yields

$$\dot{\theta}_R = 0. \tag{7}$$

As Newton's impact law may give incorrect results in complicated vibro-impact system and the method of energy dissipation impact fails to work for the system when the normal phase switch is asynchronous with the reverse of tangential micro-slip, only Poisson's impact law is applicable now. For simplicity, let $r \in (0, 1]$ be the normal coefficient of restitution. Let $P_I$ and $P_{II}$ be the normal impulse acting on the colliding bodies in the approach phase and the restitution phase, respectively. Using Poisson's impact law yields

$$P_{II} = rP_I. \tag{8}$$

Furthermore, to distinguish the cases by using the impulse, let $P_f$ be the normal impulse in the normal approach phase if the tangential micro-slip does not reverse in this phase, and let $P_*$ be the normal impulse from the very beginning of impact to the moment when the tangential micro-slip reverses. From Eqs. (5) and (6), one finds

$$P_f = \frac{\dot{\theta}_0\cos\theta_0 - \dot{x}_0}{\bar{m} + \cos^2\theta_0 + \mu\,\mathrm{sgn}(\dot{\theta}_0)\sin\theta_0\cos\theta_0}. \tag{9}$$

According to Eqs. (7) and (5a), one obtains

$$P_* = \dot{\theta}_0/[\cos\theta_0 + \mu\,\mathrm{sgn}(\dot{\theta}_0)\sin\theta_0]. \tag{10}$$

Now, the analytical relations between the pre-impact state and the post-impact state can be derived in three cases from the relation among $P_f$, $P_*$ and $r$ as follows:

(1) If $P_* < P_f$, the tangential micro-slip reverses within the normal approach phase in the impact process. According to the switch of the normal phases (approach phase and the restitution phase) and the reverse of tangential micro-slip, the impact process can be divided into three phases. They are the first approach phase from the moment when the impact begins to the reverse moment of tangential micro-slip, the second approach phase from the reverse moment of the tangential micro-slip to the end of the whole approach phase, and the restitution phase. Then, the analytical relations between the initial state and the terminal state in each phase can be determined by using the impulse-moment method.

From Eqs. (5) and (7), the initial state $(\dot{\theta}_0, \dot{x}_0)$ and the terminal state $(\dot{\theta}_R, \dot{x}_R)$ in the first approach phase, and the impulse $P_R$ acting on the colliding bodies in this phase yield

$$\begin{aligned} \dot{\theta}_R &= \dot{\theta}_0 - P_R[\cos\theta_0 + \mu\,\mathrm{sgn}(\dot{\theta}_0)\sin\theta_0] = 0, \\ \dot{x}_R &= \dot{x}_0 + \bar{m}P_R. \end{aligned} \tag{11}$$

Similarly, the initial state and the terminal state in the second approach phase satisfy

$$\begin{aligned} \dot{\theta}_I &= \dot{\theta}_R - (P_I - P_R)[\cos\theta_0 - \mu\,\mathrm{sgn}(\dot{\theta}_0)\sin\theta_0], \\ \dot{x}_I &= \dot{x}_R + \bar{m}(P_I - P_R). \end{aligned} \tag{12}$$

One can notice that the tangential friction reverses its direction in this case. Furthermore, the initial and terminal states in the restitution phase yield

$$\begin{aligned} \dot{\theta}_f &= \dot{\theta}_I - rP_I[\cos\theta_0 - \mu\,\mathrm{sgn}(\dot{\theta}_0)\sin\theta_0], \\ \dot{x}_f &= \dot{x}_I + \bar{m}rP_I, \end{aligned} \tag{13}$$

where $(\dot{\theta}_f, \dot{x}_f)$ is the terminal state in the restitution phase.

By solving Eqs. (11)–(13) in turn, the analytical relations between the pre-impact state and the post-impact state can be expressed as

$$\begin{aligned} \dot{\theta}_f = -\frac{1}{A}[\cos\theta_0 - \mu\,\mathrm{sgn}(\dot{\theta}_0)\sin\theta_0]\{&\bar{m}\dot{\theta}_0 - r\dot{\theta}_0\cos\theta_0[\cos\theta_0 - \mu\,\mathrm{sgn}(\dot{\theta}_0)\sin\theta_0] \\ &+ (1+r)\dot{x}_0[\cos\theta_0 + \mu\,\mathrm{sgn}(\dot{\theta}_0)\sin\theta_0]\}, \end{aligned} \tag{14a}$$

$$\begin{aligned} \dot{x}_f = -\frac{1}{A}\{&\dot{x}_0\cos\theta_0[\cos^2\theta_0 - \mu^2\sin^2\theta_0] + (1+r)\bar{m}\dot{\theta}_0\cos\theta_0[\cos\theta_0 - \mu\,\mathrm{sgn}(\dot{\theta}_0)\sin\theta_0] \\ &- r\bar{m}\dot{x}_0[\cos\theta_0 + \mu\,\mathrm{sgn}(\dot{\theta}_0)\sin\theta_0]\}, \end{aligned} \tag{14b}$$

where

$$A = \mu^2\sin^2\theta_0\cos\theta_0 - \cos^3\theta_0 - \bar{m}[\cos\theta_0 + \mu\,\mathrm{sgn}(\dot{\theta}_0)\sin\theta_0]. \tag{15}$$

(2) If $P_f < P_* < (1+r)P_f$, the tangential micro-slip reverses within the normal restitution phase in the impact process. Similarly, the analytical relations between the pre-impact state and the post-impact state can be determined:

$$\dot{\theta}_f = \frac{1}{B_1}[\cos\theta_0 - \mu\,\mathrm{sgn}(\dot{\theta}_0)\sin\theta_0]\{\bar{m}\dot{\theta}_0 - [\cos\theta_0 + \mu\,\mathrm{sgn}(\dot{\theta}_0)\sin\theta_0][r\dot{\theta}_0\cos\theta_0 - (1+r)\dot{x}_0]\}, \tag{16a}$$

$$\dot{x}_f = \frac{1}{B_2}\{\dot{x}_0\cos\theta_0[\cos\theta_0 + \mu\,\mathrm{sgn}(\dot{\theta}_0)\sin\theta_0] + (1+r)\bar{m}\dot{\theta}_0\cos\theta_0 - r\bar{m}\dot{x}_0\}, \tag{16b}$$

where

$$B_2 = \bar{m} + \cos\theta_0[\cos\theta_0 + \mu\,\mathrm{sgn}(\dot{\theta}_0)\sin\theta_0], \tag{17a}$$

$$B_1 = B_2[\cos\theta_0 + \mu\,\mathrm{sgn}(\dot{\theta}_0)\sin\theta_0]. \tag{17b}$$

(3) If $P_* > (1+r)P_f$, the tangential micro-slip does not reverse within the impact process, and retains its initial direction till the end of impact when two bodies separate. The analytical relations

between the pre-impact state and the post-impact state are similarly determined:

$$\dot{\theta}_f = \frac{1}{B_2}\{\bar{m}\dot{\theta}_0 + [\cos\theta_0 + \mu\,\mathrm{sgn}(\dot{\theta}_0)\sin\theta_0][(1+r)\dot{x}_0 - r\dot{\theta}_0\cos\theta_0]\}, \tag{18a}$$

$$\dot{x}_f = \frac{1}{B_2}\{(1+r)\bar{m}\dot{\theta}_0\cos\theta_0 + \dot{x}_0\cos\theta_0[\cos\theta_0 + \mu\,\mathrm{sgn}(\dot{\theta}_0)\sin\theta_0] - r\bar{m}\dot{x}_0\}. \tag{18b}$$

### 2.2. Oblique-impact relation with friction ignored

This degenerate case implies $\mu = 0$. That is, the tangential friction in the contact surface is ignored. Then, the analytical relation between the pre-impact state and the post-impact state are expressed as

$$\dot{\theta}_f = r_1\dot{\theta}_0 + r_2\dot{x}_0, \quad \dot{x}_f = r_3\dot{\theta}_0 + r_4\dot{x}_0, \tag{19}$$

where

$$\begin{aligned} r_1 &= \frac{\bar{m} - r_0\cos^2\theta_0}{\bar{m} + \cos^2\theta_0}, \quad r_2 = \frac{(1+r_0)\cos\theta_0}{\bar{m} + \cos^2\theta_0}, \\ r_3 &= \frac{(1+r_0)\bar{m}\cos\theta_0}{\bar{m} + \cos^2\theta_0}, \quad r_4 = \frac{-r_0\bar{m} + \cos^2\theta_0}{\bar{m} + \cos^2\theta_0} \end{aligned} \tag{20}$$

and $r_0$ $(0 < r_0 \leqslant 1)$ is the constant coefficient of restitution, which can be defined by any method (velocity, momentum or energy dissipation), to denote the restitution of the case of direct-impact. Because the momentums of such a pendulum-oscillator system depend on the impact angle, all the parameters $r_i$ $(i = 1, \ldots, 4)$ in Eq. (20) are the functions in impact angle.

In a recent study [30], the above cases and the corresponding analytical relations (14), (16), (18) and (19) between the pre-impact state and the post-impact state have been fully verified by using the incremental impulse method in conjunction with experiments.

## 3. Periodic motions and their stability of an oblique-impact vibrating system

This section presents the dynamics of the oblique-impacting system shown in Fig. 1 on the basis of the oblique-impact relations in Section 2, and gives some dynamic behaviors of the system under the condition of oblique-impacts.

### 3.1. Model of oblique-impact vibration

As shown in Fig. 1, the system is characterized by the distance $\Delta$ from the equilibrium position of the pendulum to that of the left surface of the mass. If the system displacements satisfy the following equation:

$$l\sin\theta - X < \Delta, \tag{21}$$

the motions of two parts are totally decoupled. If $l\sin\theta - X = \Delta$, the tip mass $M_1$ of the pendulum contacts the left surface of mass $M_2$ at a certain angle, then the oblique-impact happens.

When the motions of two parts are decoupled, the dynamic equation of the system can be written as

$$\left.\begin{aligned} &\ddot{x}_1 + 2\zeta_1\omega_0\dot{x}_1 + \omega_0^2 x = f_1\cos(\omega t + \varphi) \\ &\ddot{x}_2 + 2\zeta_2\dot{x}_2 + x_2 = f_2\cos(\omega t + \varphi) \end{aligned}\right\} \quad \text{when } \sin x_1 - x_2 < \delta, \tag{22}$$

where

$$\begin{aligned} &\omega_0 = \frac{\omega_1}{\omega_2}, \quad \zeta_1 = \frac{C_1}{2\sqrt{M_1K_1l^2}}, \quad \zeta_2 = \frac{C_2}{2\sqrt{M_2K_2}}, \quad f_1 = \frac{f_{10}\bar{\omega}^2}{K_1}, \quad f_2 = \frac{f_{20}}{K_2 l}, \\ &t = \omega_2 T, \quad \omega = \Omega/\omega_2, \quad x_1 = \theta, \quad x_2 = X/l, \quad \delta = \Delta/l \end{aligned} \tag{23}$$

are a few dimensionless variables and $\omega_1 = \sqrt{K_1/(M_1l^2)}$ and $\omega_2 = \sqrt{K_2/M_2}$ are defined as the natural frequencies of two parts, respectively.

From the analysis in Section 2, the oblique-impact within such a system features that the micro-slip or slip-reverse may occur in the tangential direction, and the relation between the pre-impact and the post-impact states cannot be expressed as a unique expression when the tangential friction is taken into consideration. This fact gives great difficulty to the analysis of the dynamics. Thus, the following treatment will be introduced as following. The analytical method will be used to study the periodic vibro-impact and its stability in the case when the tangential friction is ignored, whereas the numerical method will be used in the case when the friction is taken into account. Then, $\mu = 0$ is an essential assumption in this section.

It is assumed that the contact time in the oblique-impact process is infinitesimal compared to the time of independent motion. Let $t = 0$ be the instant when an impact starts, $(x_1(0^-), \dot{x}_1(0^-), x_2(0^-), \dot{x}_2(0^-))$ and $(x_1(0^+), \dot{x}_1(0^+), x_2(0^+), \dot{x}_2(0^+))$ be the pre-impact state and the post-impact state, respectively. From Eq. (15), one can express the relations between pre-impact state and post-impact state as

$$\left.\begin{aligned} &x_1(0^+) = x_1(0^-), \quad \dot{x}_1(0^+) = r_1\dot{x}_1(0^-) + r_2\dot{x}_2(0^-) \\ &x_2(0^+) = x_2(0^-), \quad \dot{x}_2(0^+) = r_3\dot{x}_1(0^-) + r_4\dot{x}_2(0^-) \end{aligned}\right\} \quad \text{when } \sin x_1 - x_2 = \delta, \tag{24}$$

where $r_i$ $(i = 1, \ldots, 4)$ are expressed as Eq. (20). Hence, all $r_i$, $i = 1, \ldots, 4$ are functions of impact angle $x_1(0^-)$.

The flight motion between two successive impacts can be determined through the solution of Eq. (22):

$$\begin{aligned} x_1(t) &= \bar{S}_{11}(t)x_1(0^+) + \bar{S}_{12}(t)\dot{x}_1(0^+) + \bar{S}_{13}(t)\sin\varphi + \bar{S}_{14}(t)\cos\varphi, \\ \dot{x}_1(t) &= \bar{S}_{21}(t)x_1(0^+) + \bar{S}_{22}(t)\dot{x}_1(0^+) + \bar{S}_{23}(t)\sin\varphi + \bar{S}_{24}(t)\cos\varphi, \\ x_2(t) &= \bar{S}_{31}(t)x_2(0^+) + \bar{S}_{32}(t)\dot{x}_2(0^+) + \bar{S}_{33}(t)\sin\varphi + \bar{S}_{34}(t)\cos\varphi, \\ \dot{x}_2(t) &= \bar{S}_{41}(t)x_2(0^+) + \bar{S}_{42}(t)\dot{x}_2(0^+) + \bar{S}_{43}(t)\sin\varphi + \bar{S}_{44}(t)\cos\varphi, \end{aligned} \tag{25}$$

where the expressions of $\bar{S}_{ij}(t)$, $i = 1, \ldots, 4$, $j = 1, \ldots, 4$ are listed in Appendix A.

If a specific state just ahead of an impact is given as $(x_1, \dot{x}_1, x_2, \dot{x}_2)$ and the instant is defined as $t = t_0^- = t_0^+ = 0$ and $\varphi = \varphi_0^- = \varphi_0^+$ because the duration of impact process is ignored, one can obtain all the states of the system by repeating the process expressed by Eqs. (24) and (25).

### 3.2. Analysis of period-$n-1$ oblique-impact vibration

#### 3.2.1. General case when $\mu = 0$

In this section the period-$n-1$ motions of the oblique-impact vibrating system will be analyzed in the phase space $\mathbf{R}^4 \times \mathbf{R}^+ \times \mathbf{R}^+$ with the state vector $\mathbf{X} = (x_1, \dot{x}_1, x_2, \dot{x}_2)$. By selecting the following impact section as the Poincaré section:

$$\mathbf{\Sigma} = \{(\mathbf{X}, \varphi, t) \in \mathbf{R}^4 \times \mathbf{R}^+ \times \mathbf{S} | \sin x_1 - x_2 = \delta, t = t_{\text{impact}}^-\}, \tag{26}$$

where $\mathbf{S} = \{t(\text{mod}(2n\pi/\omega)) | t \in \mathbf{R}^+\}$, and defining the following Poincaré mapping:

$$\mathbf{P} : \mathbf{\Sigma} \to \mathbf{\Sigma} \tag{27}$$

one can transform the analysis of the period-$n-1$ impact motions of the system to the analysis of the fixed points on the above Poincaré section. Obviously, the map $\mathbf{P}$ includes two sub-mapping processes $\mathbf{P}_1 : \mathbf{X}_0 \to \mathbf{X}_0^+$ and $\mathbf{P}_2 : \mathbf{X}_0^+ \to \mathbf{X}_{2n\pi/\omega}$, where $\mathbf{X}_0 = (x_{10}, \dot{x}_{10}, x_{20}, \dot{x}_{20})$, $\mathbf{X}_{2n\pi/\omega} = (x_{1,2n\pi/\omega}, \dot{x}_{1,2n\pi/\omega}, x_{2,2n\pi/\omega}, \dot{x}_{2,2n\pi/\omega})$, and $\mathbf{P}_1$ is the state transformation when an orbit in the phase space passes through the Poincaré section, $\mathbf{P}_2$ is the process of the orbit undergoing period-$n$ free vibration from the end of the impact to the time $2n\pi/\omega$ when the orbit arrives at section $\mathbf{\Sigma}$. Then, one has

$$\mathbf{P} = \mathbf{P}_2 \circ \mathbf{P}_1 : \mathbf{X}_0 \to \mathbf{X}_{2n\pi/\omega}. \tag{28}$$

From Eqs. (24) and (25), $\mathbf{P}$ can be expressed specifically as

$$\mathbf{X}_{2n\pi/\omega} = \begin{pmatrix} S_{11} & S_{12} & 0 & 0 \\ S_{21} & S_{22} & 0 & 0 \\ 0 & 0 & S_{31} & S_{32} \\ 0 & 0 & S_{41} & S_{42} \end{pmatrix} \begin{pmatrix} 1 & 0 & 0 & 0 \\ 0 & r_1 & 0 & r_2 \\ 0 & 0 & 1 & 0 \\ 0 & r_3 & 0 & r_4 \end{pmatrix} \mathbf{X}_0 + \begin{pmatrix} S_{13} & S_{14} \\ S_{23} & S_{24} \\ S_{33} & S_{34} \\ S_{43} & S_{44} \end{pmatrix} \begin{pmatrix} \sin\varphi \\ \cos\varphi \end{pmatrix}, \tag{29}$$

where $S_{ij} = \bar{S}_{ij}(2n\pi/\omega)$, $i = 1, \ldots, 4$, $j = 1, \ldots, 4$.

If the period-$n-1$ orbit exists in the phase space, the mapping $\mathbf{P}$ should satisfy

$$\mathbf{X}_{2n\pi/\omega} = \mathbf{X}_0. \tag{30}$$

Substituting the above equation into Eq. (29) and keeping $\sin x_{10} - x_{20} = \delta$ in mind, one has

$$\begin{pmatrix} r_1 S_{12} & r_2 S_{12} & S_{13} & S_{14} \\ r_1 S_{22} - 1 & r_2 S_{22} & S_{23} & S_{24} \\ r_3 S_{32} & r_4 S_{32} & S_{33} & S_{34} \\ r_3 S_{42} & r_4 S_{42} - 1 & S_{43} & S_{44} \end{pmatrix} \begin{pmatrix} \dot{x}_{10} \\ \dot{x}_{20} \\ \sin\varphi \\ \cos\varphi \end{pmatrix} = - \begin{pmatrix} (S_{11} - 1)x_{10} \\ S_{21} x_{10} \\ (S_{31} - 1)(\sin x_{10} - \delta) \\ S_{41}(\sin x_{10} - \delta) \end{pmatrix}. \tag{31}$$

Let $b_0(x_{10})$ be the determinant of the left-hand-side matrix in Eq. (31). If the condition

$$b_0(x_{10}) \neq 0 \tag{32}$$

holds, then Eq. (31) has a solution. Therefore, the impact velocities of period-$n-1$ motions are obtained as

$$\dot{x}_{10} = [b_{11}(x_{10})x_{10} + b_{12}(x_{10})(\sin x_{10} - \delta)]/b_0(x_{10}), \tag{33a}$$

$$\dot{x}_{20} = [b_{21}(x_{10})x_{10} + b_{22}(x_{10})(\sin x_{10} - \delta)]/b_0(x_{10}) \tag{33b}$$

and the corresponding excitation phase can be expressed as

$$\sin\varphi = [b_{31}(x_{10})x_{10} + b_{32}(x_{10})(\sin x_{10} - \delta)]/b_0(x_{10}), \tag{34a}$$

$$\cos\varphi = [b_{41}(x_{10})x_{10} + b_{42}(x_{10})(\sin x_{10} - \delta)]/b_0(x_{10}). \tag{34b}$$

Using the relation $\sin^2\varphi + \cos^2\varphi = 1$, one has

$$\begin{aligned}&[b_{31}^2(x_{10}) + b_{41}^2(x_{10})]x_{10}^2 + 2[b_{31}(x_{10})b_{32}(x_{10}) + b_{41}(x_{10})b_{42}(x_{10})]x_{10}(\sin x_{10} - \delta)\\ &\quad + [b_{32}^2(x_{10}) + b_{42}^2(x_{10})](\sin x_{10} - \delta)^2 = b_0^2(x_{10}),\end{aligned} \tag{35}$$

where the coefficients $b_0$ and $b_{ij}$ $(i = 1, \ldots, 4,\ j = 1, 2)$ in Eqs. (32)–(35) are listed in Appendix B.

From the above analysis, the period-$n-1$ motions can exist in the oblique-impact vibrating system governed by Eq. (22) if Eq. (32) holds and Eq. (35) has any real solution. Accordingly, all points $\mathbf{X}_0 = (x_{10}, \dot{x}_{10}, x_{20}, \dot{x}_{20}) \in \boldsymbol{\Sigma}$ satisfying Eqs. (32)–(35) are the $n-1$ fixed points on the Poincaré section. Because the impact relation described by Eq. (24) and the corresponding impact conditions are non-linear, it is not possible to obtain any analytical solution of Eq. (35).

*3.2.2. Case when $\zeta_1 = \zeta_2 = 0$ and $f_2 = 0$*

For the sake of simplicity, this section focuses on a special case when $\zeta_1 = \zeta_2 = 0$ and $f_2 = 0$ are assumed. In this case, all $S_{ij}$, $i = 1, \ldots, 4$, $j = 1, \ldots, 4$ can be recast as

$$\begin{aligned}&S_{11} = \cos(2n\pi\omega_0/\omega), \quad S_{12} = \frac{1}{\omega_0}\sin(2n\pi\omega_0/\omega), \quad S_{13} = \frac{f_1\omega}{\omega_0(\omega_0^2 - \omega^2)}\sin(2n\pi\omega_0/\omega),\\ &S_{14} = \frac{f_1}{\omega_0^2 - \omega^2}[1 - \cos(2n\pi\omega_0/\omega)], \quad S_{21} = -\omega_0^2 S_{12}, \quad S_{22} = S_{11}, \quad S_{23} = -\omega S_{14},\\ &S_{24} = \omega_0^2 S_{13}/\omega, \quad S_{31} = \cos(2n\pi/\omega), \quad S_{32} = \sin(2n\pi/\omega),\\ &S_{33} = 0, \quad S_{34} = 0, \quad S_{41} = -S_{32}, \quad S_{42} = S_{31}, \quad S_{43} = 0, \quad S_{44} = 0.\end{aligned} \tag{36}$$

By substituting Eq. (36) into Eqs. (32)–(35), recasting and simplifying the result, one can prove that the period-$n-1$ oblique-impact motions exist in the cases when the following inequality holds:

$$\frac{2(1+r)\bar{m}f_1^2\omega\cos x_{10}\sin(2n\pi/\omega)[\cos(2n\pi\omega_0/\omega) - 1]}{(\bar{m} + \cos^2 x_{10})(\omega_0^2 - \omega^2)^2} \neq 0 \tag{37}$$

and the following equation:

$$\begin{aligned}x_{10}^2 + \frac{2\tan(n\pi/\omega)\cos x_{10}}{\bar{m}\omega_0\tan(n\pi\omega_0/\omega)}(\sin x_{10} - \delta)x_{10} + \frac{\tan^2(n\pi/\omega)}{\bar{m}^2}\left[\frac{\cos^2 x_{10}}{\omega_0^2\tan^2(n\pi\omega_0/\omega)}\right.\\ \left. + \frac{(1-r)^2(\bar{m} + \cos^2 x_{10})^2}{(1+r)^2\omega^2\cos^2 x_{10}}\right](\sin x_{10} - \delta)^2 = \frac{f_1^2}{(\omega_0^2 - \omega^2)^2}\end{aligned} \tag{38}$$

has at least one real solution. The corresponding impact velocities and excitation phase yield

$$\dot{x}_{10} = \frac{[(1-r)\bar{m} + 2\cos^2 x_{10}]\tan(n\pi/\omega)}{(1+r)\bar{m}\cos x_{10}}(\sin x_{10} - \delta), \tag{39a}$$

$$\dot{x}_{20} = -\tan(n\pi/\omega)(\sin x_{10} - \delta), \tag{39b}$$

$$\sin\varphi = -\frac{(1-r)(\omega_0^2 - \omega^2)(\bar{m} + \cos^2 x_{10})\tan(n\pi/\omega)}{(1+r)\bar{m}f_1\omega\cos x_{10}}(\sin x_{10} - \delta), \tag{40a}$$

$$\cos\varphi = \frac{(\omega_0^2 - \omega^2)}{f_1}\left[x_{10} + \frac{\tan(n\pi/\omega)\cos x_{10}}{\bar{m}\omega_0\tan(n\pi\omega_0/\omega)}(\sin x_{10} - \delta)\right]. \tag{40b}$$

Therefore, if Eq. (37) holds, the excitation frequency must satisfy $\omega \neq n/m$ and $\omega \neq \omega_0$ (where $m$ is an arbitrary positive integer), and mass $M_1$ cannot contact mass $M_2$ at the horizontal position of the pendulum in Fig. 1, namely, $\theta \neq 2k\pi + \pi/2$. To gain an insight into Eq. (38), a numerical study will be given in Section 4 to show transition of its real solution with variation of system parameters.

### 3.3. Stability analysis of period-$n-1$ oblique-impact vibration

The objective of this subsection is to study the stability of period-$n-1$ motions determined in the previous subsection. For this purpose, the method of Poincaré mapping will be used so that attention will be paid to the stability analysis of the fixed points of the Poincaré mapping.

Now, a new fixed point $\mathbf{Y} = (x_{10}, \dot{x}_{10}, \dot{x}_{20}, \varphi)$ is defined from Eq. (31), which can be recast as

$$\begin{aligned}
&(S_{11}-1)x_{10} + r_1S_{12}\dot{x}_{10} + r_2S_{12}\dot{x}_{20} + S_{13}\sin\varphi + S_{14}\cos\varphi = 0,\\
&S_{21}x_{10} + (r_1S_{22}-1)\dot{x}_{10} + r_2S_{22}\dot{x}_{20} + S_{23}\sin\varphi + S_{24}\cos\varphi = 0,\\
&(S_{31}-1)\sin x_{10} + r_3S_{32}\dot{x}_{10} + r_4S_{32}\dot{x}_{20} + S_{33}\sin\varphi + S_{34}\cos\varphi - (S_{31}-1)\delta = 0,\\
&S_{41}\sin x_{10} + r_3S_{42}\dot{x}_{10} + (r_4S_{42}-1)\dot{x}_{20} + S_{43}\sin\varphi + S_{44}\cos\varphi - S_{41}\delta = 0.
\end{aligned} \tag{41}$$

The Jacobian of Eq. (41) at this fixed point reads

$$\mathbf{DP} = \begin{pmatrix} a_{11} & a_{12} & a_{13} & a_{14}\\ a_{21} & a_{22} & a_{23} & a_{24}\\ a_{31} & a_{32} & a_{33} & a_{34}\\ a_{41} & a_{42} & a_{43} & a_{44}\end{pmatrix}. \tag{42}$$

The entries in the above matrix are

$$\begin{aligned}
&a_{11} = S_{11} - 1 + S_{12}(r_{1,x_{10}}\dot{x}_{10} + r_{2,x_{10}}\dot{x}_{20}), \quad a_{12} = r_1S_{12}, \quad a_{13} = r_2S_{12}, \quad a_{14} = S_{13}\cos\varphi - S_{14}\sin\varphi,\\
&a_{21} = S_{21} + S_{22}(r_{1,x_{10}}\dot{x}_{10} + r_{2,x_{10}}\dot{x}_{20}), \quad a_{22} = r_1S_{22} - 1, \quad a_{23} = r_2S_{22}, \quad a_{24} = S_{23}\cos\varphi - S_{24}\sin\varphi,\\
&a_{31} = (S_{31}-1)\cos x_{10} + S_{32}(r_{3,x_{10}}\dot{x}_{10} + r_{4,x_{10}}\dot{x}_{20}), \quad a_{32} = r_3S_{32}, \quad a_{33} = r_4S_{32},\\
&a_{34} = S_{33}\cos\varphi - S_{34}\sin\varphi,\\
&a_{41} = S_{41}\cos x_{10} + S_{42}(r_{3,x_{10}}\dot{x}_{10} + r_{4,x_{10}}\dot{x}_{20}), \quad a_{42} = r_3S_{42}, \quad a_{43} = r_4S_{42} - 1,\\
&a_{44} = S_{43}\cos\varphi - S_{44}\sin\varphi,
\end{aligned} \tag{43}$$

where $r_{i,x_{10}}$ $(i = 1, \ldots, 4)$ represent the derivative of $r_i$ with respect to $x_{10}$:

$$r_{1,x_{10}} = \frac{2\bar{m}(r+1)\sin x_{10}\cos x_{10}}{(\bar{m}+\cos^2 x_{10})^2}, \quad r_{2,x_{10}} = \frac{(r+1)\sin x_{10}(\cos^2 x_{10}-\bar{m})}{(\bar{m}+\cos^2 x_{10})^2},$$
$$r_{3,x_{10}} = \bar{m}r_{2,x_1}, \quad r_{4,x_{10}} = -r_{1,x_{10}} \tag{44}$$

$\sin\varphi$ and $\cos\varphi$ can be expressed in terms of $x_{10}$ according to Eq. (34) or Eq. (40). Then, the characteristic equation of the Jacobian given in Eq. (42) reads

$$\lambda^4 + J_3\lambda^3 + J_2\lambda^2 + J_1\lambda + J_0 = 0, \tag{45}$$

where the coefficients $J_i$ $(i = 0, \ldots, 3)$ are listed in Appendix C.

The stability of the fixed points can be judged from the following roots of Eq. (45)

$$\lambda_{1,2} = \frac{\sqrt{A}}{2} - \frac{J_3}{4} \pm \frac{1}{2}\sqrt{D + \frac{-8J_1 + 4J_2J_3 - J_3^3}{4\sqrt{A}}},$$
$$\lambda_{3,4} = -\frac{\sqrt{A}}{2} - \frac{J_3}{4} \pm \frac{1}{2}\sqrt{D - \frac{-8J_1 + 4J_2J_3 - J_3^3}{4\sqrt{A}}}, \tag{46}$$

where

$$A = \frac{(\sqrt{B}+G)^{1/3}}{3\cdot 2^{1/3}} + \frac{J_3^2}{4} - \frac{2J_2}{3} + \frac{2^{1/3}(12J_0 + J_2^3 - 3J_1J_3)}{3(\sqrt{B}+G)^{1/3}},$$
$$D = -\frac{(\sqrt{B}+G)^{1/3}}{3\cdot 2^{1/3}} + \frac{J_3^2}{4} - \frac{2J_2}{3} - \frac{2^{1/3}(12J_0 + J_2^3 - 3J_1J_3)}{3(\sqrt{B}+G)^{1/3}},$$
$$B = G^2 - 4(12J_0 + J_2^3 - 3J_1J_3)^3,$$
$$G = 2J_2^3 - 9J_1J_2J_3 + 27J_1^2 + 27J_0J_3^2 - 72J_0J_2. \tag{47}$$

If all the roots $\lambda_i$, $i = 1, \ldots, 4$, are within a unit circle, the periodic motion corresponding to the fixed point is asymptotically stable. If any $\lambda_i$ is out of the unit circle, the period motion is unstable. Furthermore, the types of bifurcation can be clarified as the following:

1. The saddle-node bifurcation occurs in the case when one of the roots of Eq. (45) is passing through the unit circle in the positive direction of the real axis;
2. The period doubling bifurcation occurs in the case when one of the roots of Eq. (45) is passing through the unit circle in the negative direction of the real axis;
3. The Hopf bifurcation may occur in the case when a pair of conjugated roots of Eq. (45) is passing through the unit circle.

## 4. Case studies

In this section, some numerical results are given to intuitively show the existence and the stability of periodic motions of the oblique-impact vibrating system composed of a spring–pendulum and a mass–spring oscillator, and the long-term dynamic behavior of the system. The

following two Poincaré sections, which are defined by the impact section or the excitation periodic phase section as follows, will be used:

$$\mathbf{\Sigma}_{\text{Impact}} = \{(x_1, \dot{x}_1, x_2, \dot{x}_2, \varphi) | \sin x_1 - x_2 = \delta\}, \tag{48a}$$

$$\mathbf{\Sigma}_{\text{Time}} = \{(x_1, \dot{x}_1, x_2, \dot{x}_2, t) | \bmod(t, T) = 0\}. \tag{48b}$$

Except $\varphi$ and $t$, the transition of each entry in $(x_1, \dot{x}_1, x_2, \dot{x}_2)$ can represent the transition of the steady state motions of the system. Hence, $x_1$, the angle displacement of the pendulum, is chosen to describe the transition of the steady state motions on the Poincaré sections. In the numerical emulation, Eqs. (19) and (20) are used to describe the oblique-impact relation when the friction is ignored, whereas Eqs. (14), (16), and (18) are used when the friction is taken into account. In the numerical simulation, 600 periods of excitation are used to arrive at the steady state motion and only the results of the last 100 periods are recorded for analysis.

### 4.1. Simplified cases

In the simplified cases analyzed in Section 3.2.2, the system is assumed to have no viscous damping and no tangential friction in the impact surface, and to be subject to a harmonic moment excitation on the pendulum. That is, $\mu = 0$, $\zeta_1 = \zeta_2 = 0$, $f_2 = 0$. By selecting the parameters $\delta = 0.5$, $\bar{m} = 0.6$, $\omega_0 = 2$ and $r = 0.8$, the periodic vibro-impacts can be computed through Eqs. (37)–(40), and the corresponding stability can be determined from the eigenvalues of the Jacobian of the Poincaré mapping.

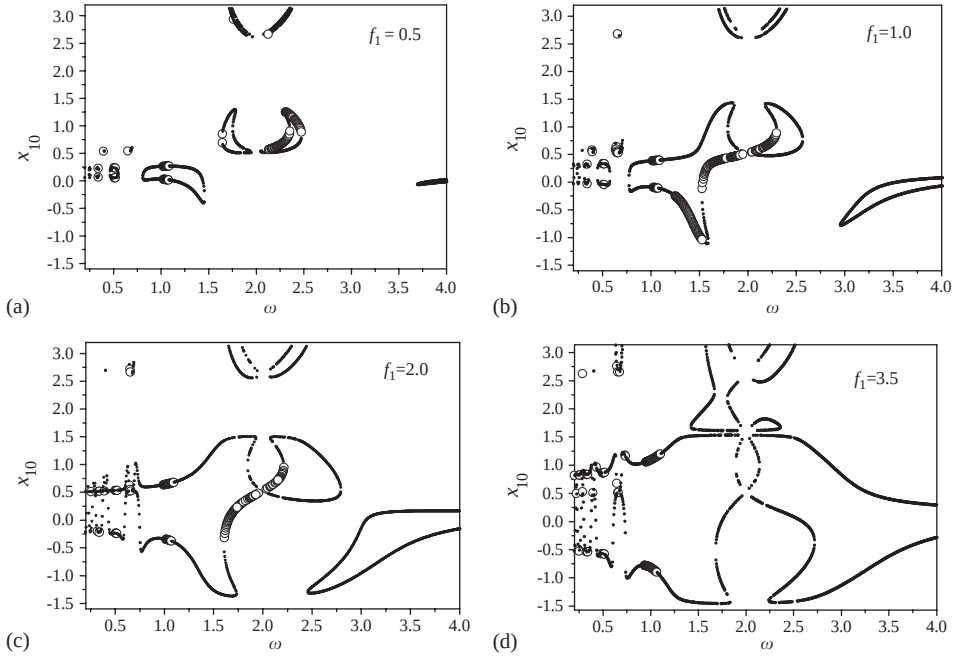


Fig. 2. The existence and stability of the period-1 – 1 motions of an oblique-impact vibrating system (◦, stable; •, unstable).

The existence and the stability of period-1 − 1 and period-2 − 1 vibro-impacts of the simplified system are shown in Figs. 2 and 3, respectively. Some phenomena can be observed from those figures: (1) The appearance of periodic motions depends on the strict values of some system parameters. If $(\omega, f_1)$ is fixed, whether the periodic motions occur depends on the value of $x_{10}$ and the state point $(x_{10}, \dot{x}_{10}, \dot{x}_{20}, \varphi)$, which is decided by $x_{10}$, in Poincaré section. For example, when $(\omega, f_1) = (0.65, 0.95)$, a stable period-1 − 1 motion occurs when $x_{10} = 0.5369$, and an unstable period-2 − 1 motion occurs when $x_{10} = 0.3300$. (2) When the excitation frequency $\omega$ is fixed, the regions where the periodic motions occur become larger with an increase of the excitation amplitude $f_1$, and then some separate regions can meet together. (3) The complicated bifurcations occur in the transition of the periodic motions with the variation of $\omega$ and $f$. For instance, when $f_1$ takes a large value, the transition between stability and instability occurs again and again when $\omega$ increases from 0.2 to 1.2.

The transition of the stable states on the Poincaré section with variation of excitation frequency is shown in Fig. 4 when other parameters and initial conditions of the system are fixed. It is shown that some non-linear phenomena such as various periodic motions, chaotic motions, jumps, phase locking and correlative bifurcations occur when the excitation frequency changes. Furthermore, there exist some period-$m$ motions, which undergo period-doubling bifurcation and then become chaotic motions, in some narrow frequency ranges in Fig. 4. As the illustrative motions of the simplified system, two typical period-1 − 1 motions with different phase trajectories, and a

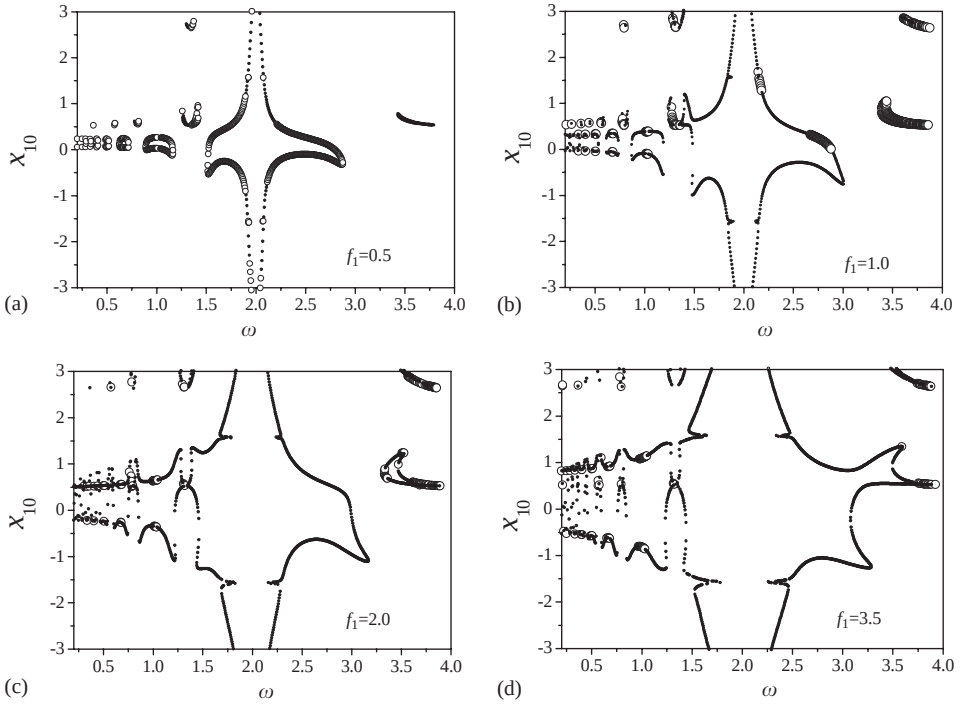


Fig. 3. The existence and stability of the period-2 − 1 motions of an oblique-impact vibrating system (◦, stable; •, unstable).

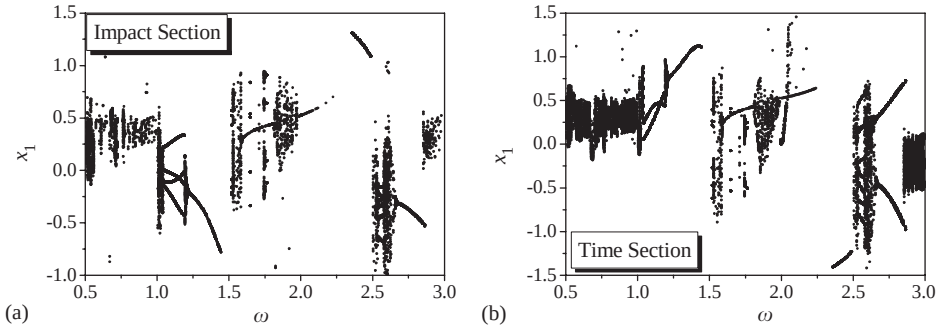


Fig. 4. The transition of the stable states on the Poincaré section with variation of excitation frequency when $\mu = 0$, $\zeta_1 = \zeta_2 = 0$, $f_1 = 1.0$, $f_2 = 0$ for the initial state $(0, 0.5, 0, 0)$. (a) Poincaré impact section; (b) Poincaré excitation phase section.

period-$2-1$ motion are shown in Fig. 5. Obviously, it is very difficult to realize the period-$n-1$ motions within the parameter region in Figs. 2 and 3. Even the initial state, which leads to a stable periodic motion in Figs. 2 and 3, may give an uncertain result if any tiny errors exist in the system parameters.

Other types of stable periodic motions may occur when the condition for period-$n-1$ motions does not hold. For example, the stable period-$1-2$ impact motions can easily occur when $f$ is less than the natural frequency of the system. Several typical low-order stable period-$m-n$ motions are shown in Fig. 6. Similar to the period-$n-1$ motions, the period-$m-n$ impact motions are also sensitive to the change of system parameters. That is, even a tiny perturbation in a system parameter may change the type or the stability of the motions. In summary, the periodic oblique-impact motions seem to be some isolated "islands" among the ubiquitous non-periodic motions.

### 4.2. General cases

#### 4.2.1. Cases with viscous damping involved, but tangential friction ignored

This section deals with the cases when the viscous damping is involved but the tangential friction in contact surface is ignored. When the system involves viscous damping, the free vibro-impact arising from different initial states will be gradually damped out so that the long-term dynamic behavior of damped system are insensitive to the initial state in contrast with the system without damping. Besides the physical parameters of the system, the long-term behaviors are mainly determined by the frequency and amplitude of the excitation. Compared with the cases in Section 4.1, a harmonic force excitation on the oscillator is added in this subsection.

The transition of the steady state behaviors with variation of the excitation frequency for different damping ratios and different excitation amplitudes are shown in Fig. 7. In the cases with given parameters and a small excitation amplitude acting on the oscillator, the figure shows that most non-periodic motions can become periodic motions when the damping ratio increases from $\zeta_1 = \zeta_2 = 0.01$ in Fig. 7(a) to $\zeta_1 = \zeta_2 = 0.1$ in Fig. 7(b), and many bifurcations in the cases with no damping or small damping disappear when the damping increases. Then, it is possible to realize the expected periodic vibro-impacts by adjusting damping and excitation. When the damping is fixed but the excitation amplitude $f_2$ increases in Fig. 7(c), it is shown that the transition of steady

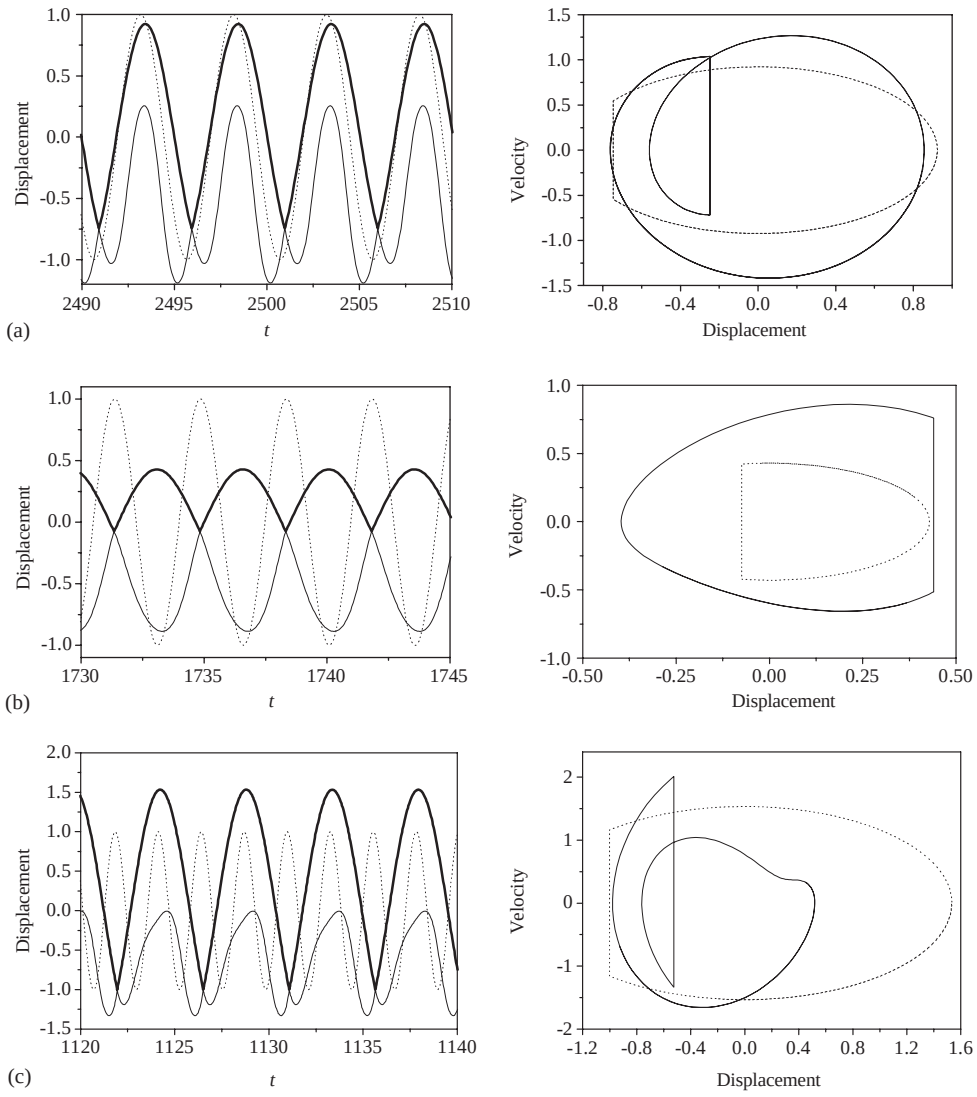


Fig. 5. The period-$n-1$ motions when $\mu = 0$, $\zeta_1 = \zeta_2 = 0$, $f_2 = 0$ for the initial state $(0, 0.5, 0, 0)$; where the thick or thin solid curve represent $x_2$ or $\sin x_1 - \delta$ and the dashed one represents $\cos \omega t$ in the left figures of the time history of displacement, the solid curve represents the phase trajectory $x_1 - \dot{x}_1$ and the dashed one represents the phase trajectory $x_2 - \dot{x}_2$ in right figures. (a) A period-$1-1$ motion when $f_1 = 1.0$, $\omega = 1.25$; (b) A period-$1-1$ motion when $f_1 = 1.0$, $\omega = 1.8$; (c) A period-$2-1$ motion when $f_1 = 1.5$, $\omega = 2.75$.

state motions is more complex than the case with small excitation amplitude $f_2$, and the parameter regions where the unstable motions occur become larger simultaneously.

*4.2.2. Cases with viscous damping and the tangential friction involved simultaneously*

This subsection deals with the cases when the viscous damping and the tangential friction in contact surface are taken into consideration simultaneously. As a comparison, except the

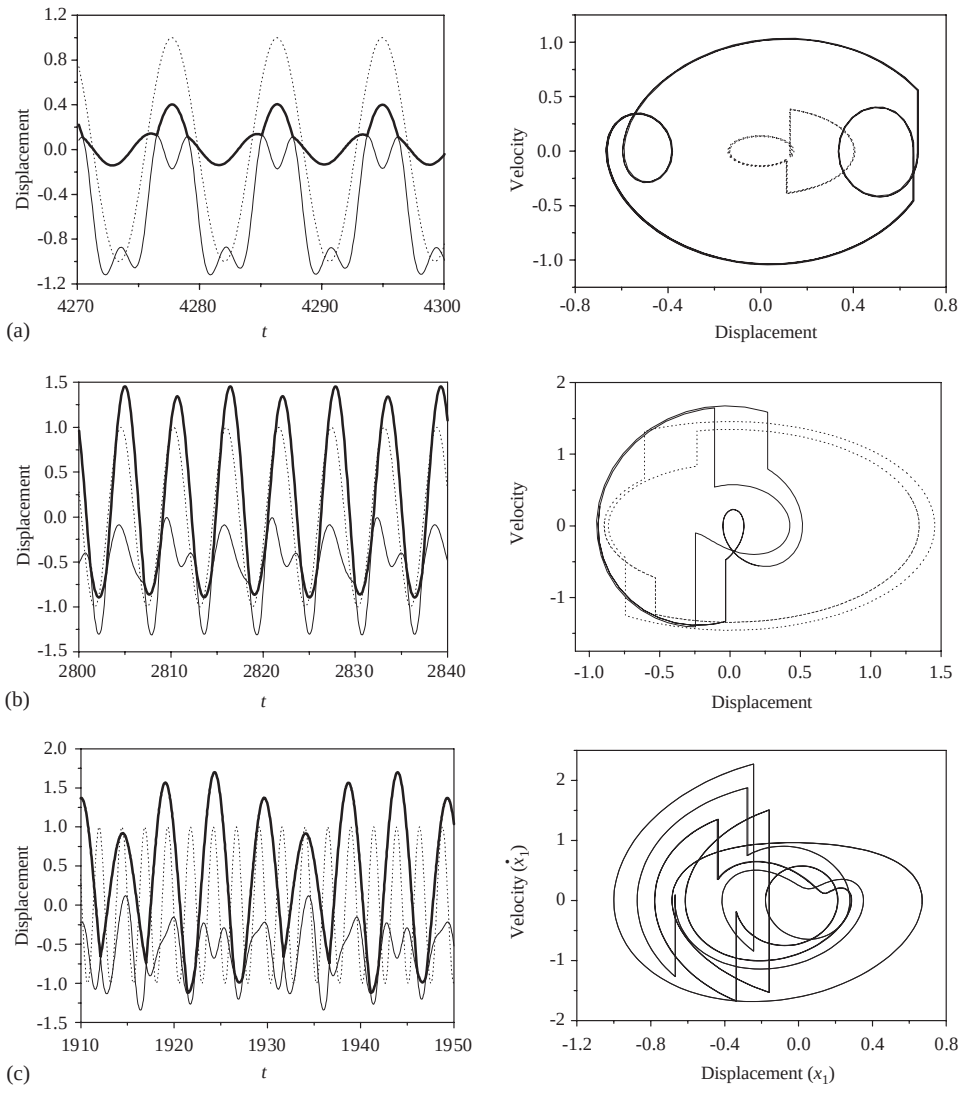


Fig. 6. Some typical examples of the low-order periodic $m-n$ motions for the initial state $(0, 0.5, 0, 0)$, where the thick or thin solid curve represent $x_2$ or $\sin x_1 - \delta$ and the dashed one represents $\cos \omega t$ in the left figures of the time history of displacement, the solid curve represents the phase trajectory $x_1 - \dot{x}_1$ and the dashed one represents the trajectory $x_2 - \dot{x}_2$ in the right figures. (a) A period-$1-2$ motion when $f_1 = 2.3$, $\omega = 0.73$; (b) A period-$2-4$ motion when $f_1 = 1.0$, $\omega = 1.1$; (c) A period-$8-6$ motion when $f_1 = 1.0$, $\omega = 2.56$; only $x_1 - \dot{x}_1$ is shown in right figure.

coefficient of the tangential friction that increases from $\mu = 0$ to $\mu = 0.5$, the same simulation parameters in Fig. 4 are selected in order to study the influence of the friction on the characteristic of steady state motions of the system. Then, the transition of the characteristic of steady state motions with variation of the excitation frequency is shown in Fig. 8(a). As shown in Fig. 4, similar non-linear phenomena, such as periodic motions, bifurcations and chaotic motions, are shown in Fig. 8(a). Furthermore, the complex motions such as period-$2-2$, period-$6-6$,

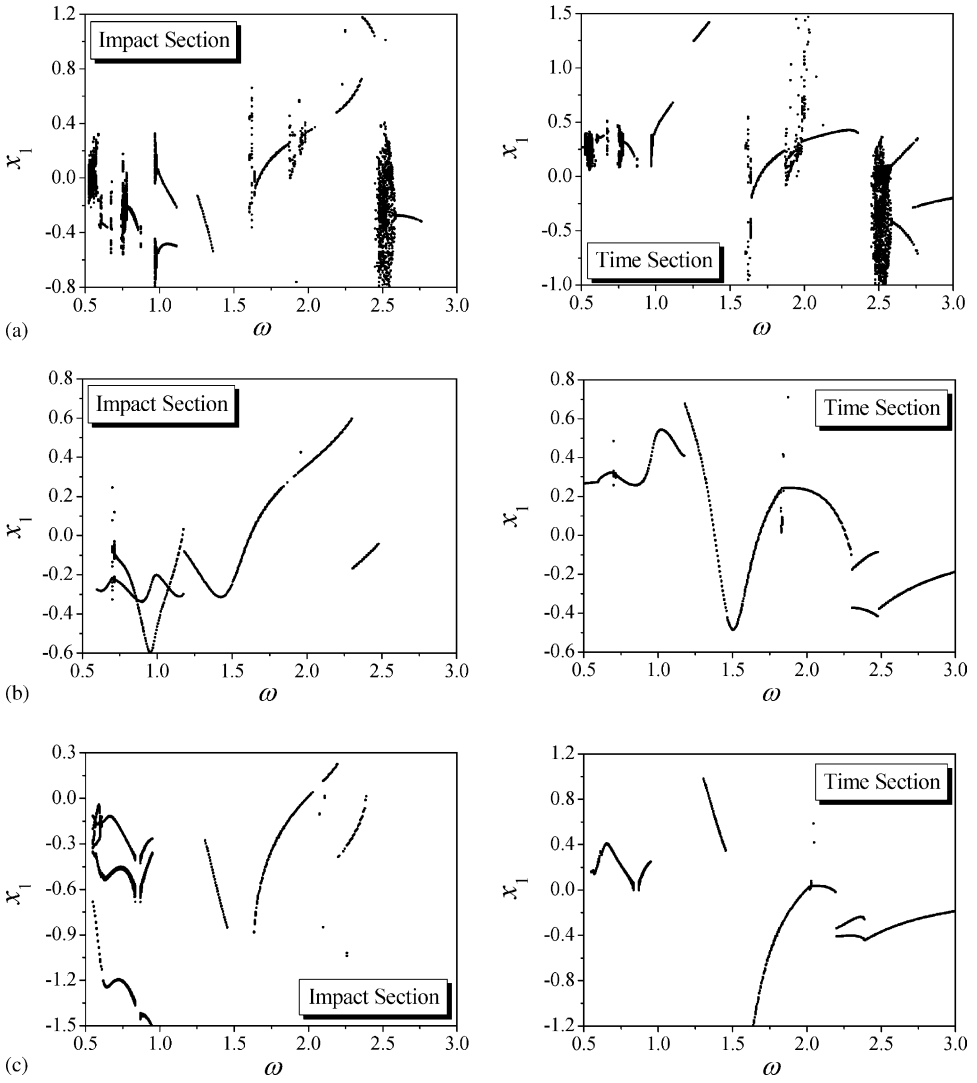


Fig. 7. The transition of the long-term dynamic behavior with variation of the excitation frequency for different damping ratios, with the system parameters $\bar{m} = 0.6,\ \omega_0 = 2,\ r = 0.8,\ \delta = 0.5$ and the initial state $(0, 0.5, 0, 0)$, where the left figures are the Poincaré impact section and the right figures the Poincaré excitation phase section. (a) System parameters: $\mu = 0,\ \zeta_1 = \zeta_2 = 0.01,\ f_1 = 1.0,\ f_2 = 0.5$; (b) System parameters: $\mu = 0,\ \zeta_1 = \zeta_2 = 0.1,\ f_1 = 1.0,\ f_2 = 0.5$; (c) System parameter: $\mu = 0,\ \zeta_1 = \zeta_2 = 0.1,\ f_1 = 1.0,\ f_2 = 1.5$.

period-4 − 5 and period-8 − 10 motions are observed in the enlarged figures. By increasing the coefficient of viscous damping to $\zeta_1 = \zeta_2 = 0.01$ and letting $f_2 = 0.5$, the transitions of the steady state motions with variation of the excitation frequency when $\mu = 0.4$ and $\mu = 0.8$ are shown in Fig. 8(b) and 8(c), respectively. These figures show that the friction can influence the behaviors of the system to some extent. For instance, the stability of the steady state motions in some

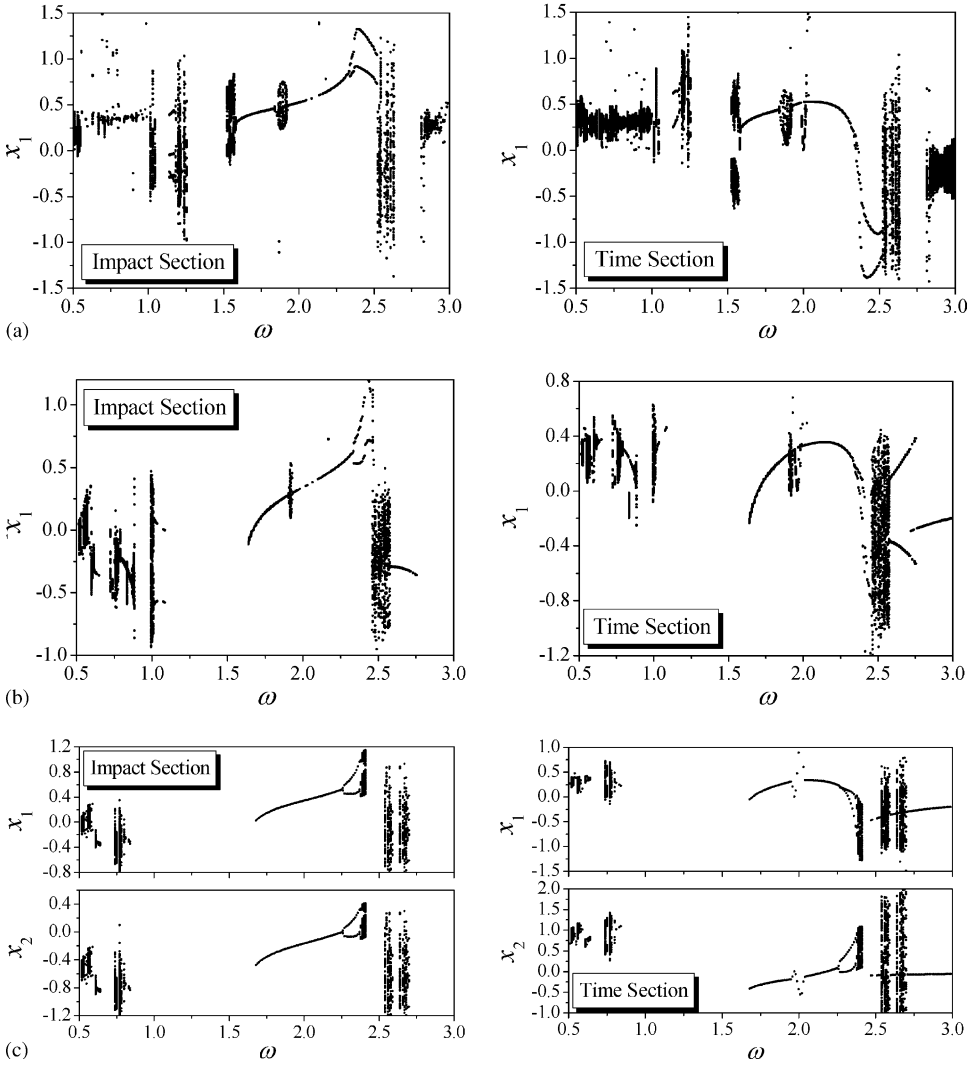


Fig. 8. The transition of the long-term dynamic behavior with variation of the excitation frequency for different coefficients of tangential friction, with the system parameters $\bar{m} = 0.6$, $\omega_0 = 2$, $r = 0.8, \delta = 0.5$ and the initial state $(0, 0.5, 0, 0)$, where the left figures are the Poincaré impact section and the right figures the Poincaré excitation phase section. (a) System parameters: $\mu = 0.5$, $\zeta_1 = \zeta_2 = 0$, $f_1 = 1.0$, $f_2 = 0$: The figure can be contrasted with Fig. 4. (b) System parameters: $\mu = 0.4$, $\zeta_1 = \zeta_2 = 0.01$, $f_1 = 1.0$, $f_2 = 0.5$. (c) System parameters: $\mu = 0.8$, $\zeta_1 = \zeta_2 = 0.01$, $f_1 = 1.0$, $f_2 = 0.5$.

parameter regions is changed and the region where the periodic motions occur becomes larger or smaller. For example, the stable period-1 $-$ 1 motions near $\omega = 1.4$ and the stable period-2 $-$ 1 motions near $\omega = 2.7$ in Fig. 7(a) disappear when the friction increases, whereas a new stable period-1 $-$ 1 motion near $\omega = 2.2$ is observed in Fig. 8(b) and 8(c). All the simulation results indicate that the influence of the friction on the system dynamics is less important than that of the

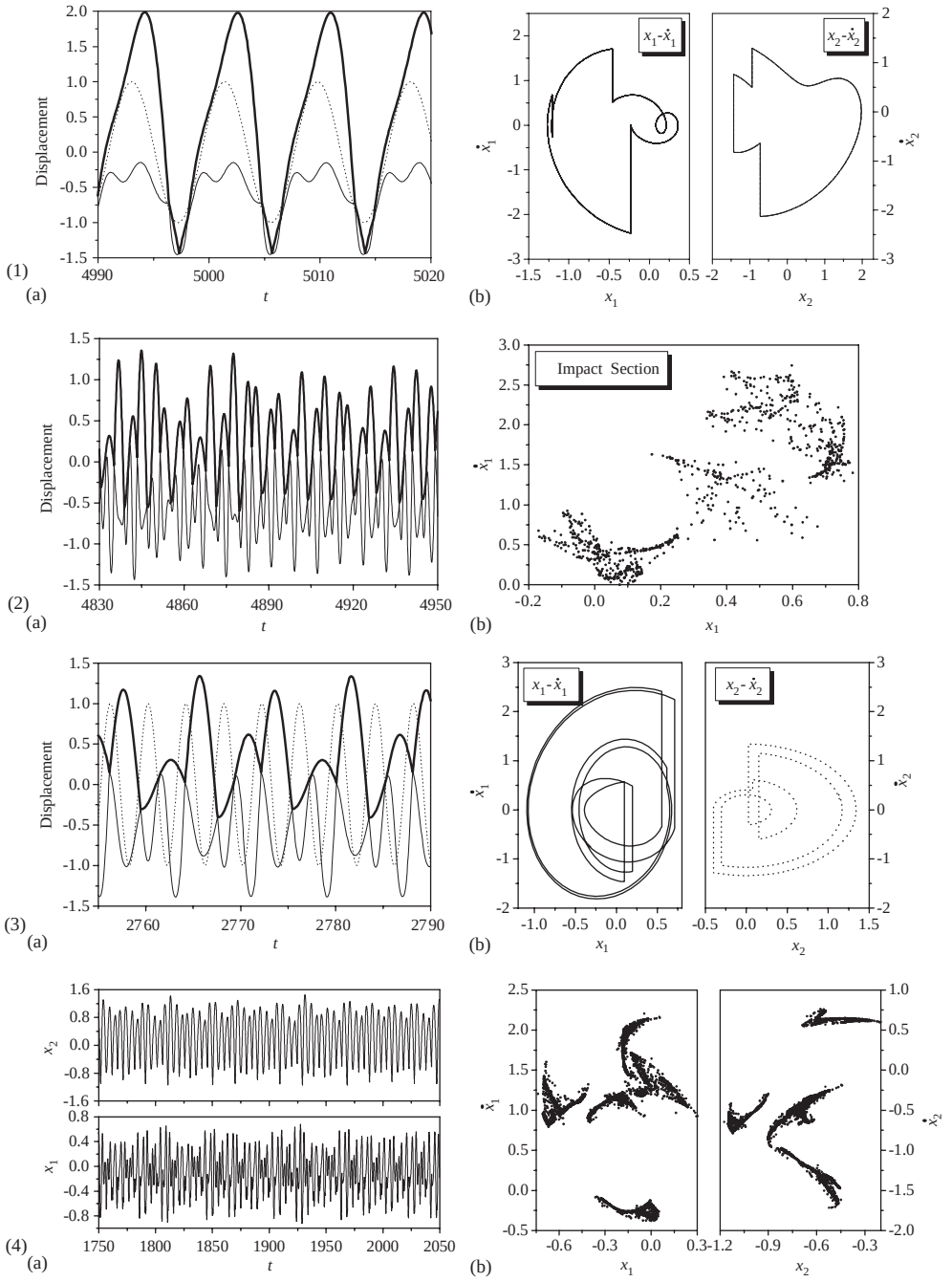


Fig. 9. Some typical motions of the oblique-impact vibrating system for system parameters $\bar{m} = 0.6$, $\omega_0 = 2$, $r = 0.8$, $\delta = 0.5$ and the initial state $(0, 0.5, 0, 0)$, where the thick or thin solid curve represents $x_2$ or $\sin x_1 - \delta$ and the dashed one represents $\cos \omega t$ in figure (a). (1) A periodic-$1-3$ motion when $\mu = 0.0$, $\zeta_1 = \zeta_2 = 0.1$, $f_1 = 1.0$, $f_2 = 1.5$, $\omega = 0.75$: (a) time history of displacement; (b) phase trajectory. (2) A chaotic motion when $\mu = 0.5$, $\zeta_1 = \zeta_2 = 0$, $f_1 = 1.0$, $f_2 = 0$, $\omega = 1.545$: (a) time history of displacement; (b) Poincaré impact section. (3) A periodic-$4-5$ motion when $\mu = 0.5$, $\zeta_1 = \zeta_2 = 0$, $f_1 = 1.0$, $f_2 = 0$, $\omega = 1.5752$: (a) time history of displacement; (b) phase trajectory. (4) A chaotic motion when $\mu = 0.4$, $\zeta_1 = \zeta_2 = 0.01$, $f_1 = 1.0$, $f_2 = 0.5$, $\omega = 2.55$: (a) time history of displacement; (b) Poincaré impact section.

damping. The variation of the damping can change the behavior of the system in large regions, whereas most steady state motions remain with their behaviors when the friction varies. As an example of general cases, Fig. 9 shows several typical periodic motions in the cases when the damping or the friction is taken into account.

As shown in Figs. 7 and 8, the characteristics of the system dynamics are observed simultaneously in the impact section and the excitation phase section when stable period-$m-n$ vibro-impacts or non-periodic vibro-impacts occur. When the motions of two sub-systems are decoupled, the general motions of the system subject to the excitation, such as the periodic motions in the case with or without damping, or the quasi-periodic motion in the case without damping, can happen independently when the excitation parameters vary. If the system is totally undamped, the phenomenon of sporadic vibro-impacts is observed in the numerical results. This phenomenon, shown in Fig. 10, indicates that the mass reaches the steady state motion after a finite number of sporadic impacts, but the pendulum remains its quasi-periodic motion forever, and the grazing impact occurs between two colliding bodies but no energy is transferred after the mass reaches the steady state motion.

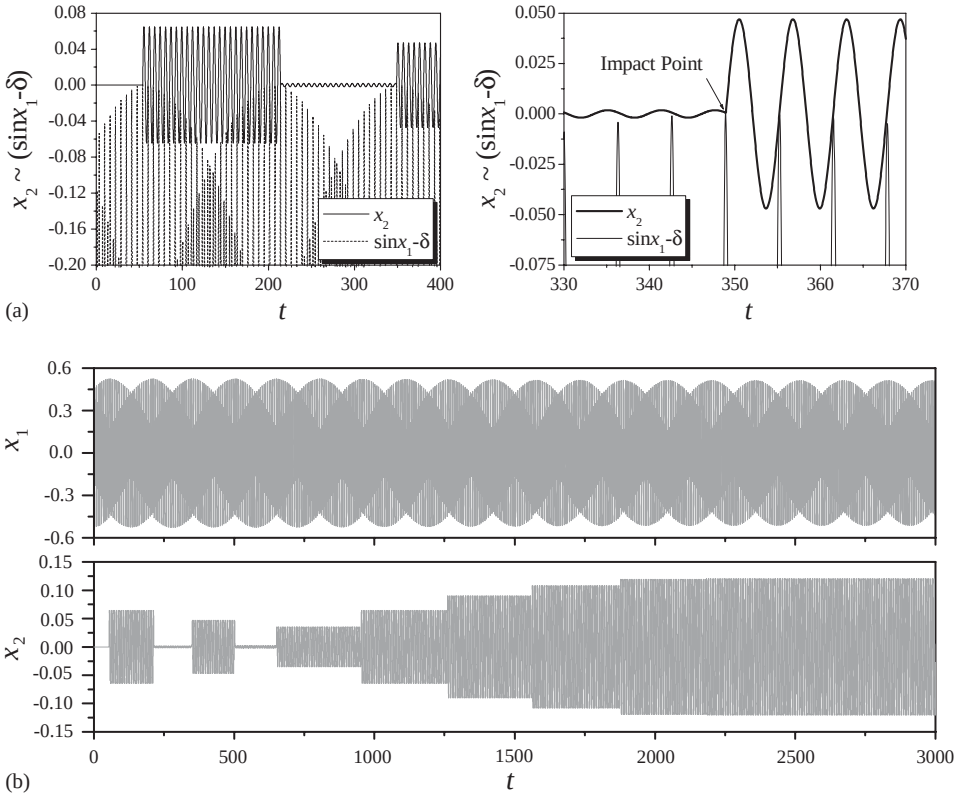


Fig. 10. The sporadic impacts ahead of a steady state periodic motion when $\bar{m} = 0.6$, $\omega_0 = 2$, $r = 0.8$, $\delta = 0.5$, $\zeta_1 = \zeta_2 = 0$, $f_1 = 1.0$, $f_2 = 0$, $\omega = 2.98$, $\mu = 0.3$, with the initial state $(0, 0.5, 0, 0)$: (a) The time history of the relatively displacement of the pendulum and the mass (left figure, $t \in (0–400)$) and the impact position (right figure, which is the zoomed view of the left figure); (b) The time–displacement history of the pendulum and the mass.

## 5. Conclusions

The present work focuses on the dynamics of an oblique-impact vibrating system composed of a spring–pendulum and a mass–spring oscillator. Specifically, the relations between the pre-impact state and the post-impact state are analyzed first upon an assumption of instantaneous oblique impacts. Then, the dynamic equation of such an oblique-impact vibrating system is established, the existence and the stability of the periodic motions are analyzed and a series of analytical solutions is obtained in the simplified cases. Furthermore, the transitions of the steady state motions of the system with the variation of excitation, damping and friction are numerically studied.

In the case of oblique-impacts, the coefficient of restitution cannot be considered as a constant according to the investigation in the paper. Meanwhile, the relations between the pre-impact state and the post-impact state are directly associated with the impact angle and the coefficient of contact–friction between impacting bodies. Because of the complexity of the impact relations, the analytical solutions of such a simple oblique-impact vibrating system can be derived only when some special conditions hold. If any stable periodic motion of such an oblique-impact vibrating system is expected, the system parameters and initial states must be carefully selected. Furthermore, rich dynamic behaviors, such as stability transitions, bifurcations and chaotic motions, can be observed in the numerical results.

## Acknowledgements

This research was supported in part by the National Natural Science Foundation of China under the grant No. 59905010, and in part by the Scientific Research Start-up Fund for the Returned Faculty of Ministry of Education. The second author wishes to acknowledge the support of the Royal Society via a BP Amoco Research Fellowship to his visit hosted by Professor S.R. Bishop at UCL.

## Appendix A

$$\bar{S}_{11}(t) = \mathrm{e}^{-\zeta_1\omega_0 t}\left(\frac{\zeta_1\omega_0}{\omega_d}\sin\omega_d t + \cos\omega_d t\right), \tag{A.1}$$

$$\bar{S}_{12}(t) = \frac{\mathrm{e}^{-\zeta_1\omega_0 t}}{\omega_d}\sin\omega_d t, \tag{A.2}$$

$$\begin{aligned}\bar{S}_{13}(t) = {} & \frac{f_1\omega\mathrm{e}^{-\zeta_1\omega_0 t}}{H}\left[\frac{(\omega_0^2-\omega^2)-2\zeta_1^2\omega_0^2}{\omega_d}\sin\omega_d t - 2\zeta_1\omega_0\cos\omega_d t\right] \\ & - \frac{f_1}{H}[(\omega_0^2-\omega^2)\sin\omega t - 2\zeta_1\omega\omega_0\cos\omega t],\end{aligned} \tag{A.3}$$

$$\bar{S}_{14}(t) = -\frac{f_1 e^{-\zeta_1\omega_0 t}}{H}\left[\frac{\zeta_1\omega_0}{\omega_d}(\omega_0^2+\omega^2)\sin\omega_d t + (\omega_0^2-\omega^2)\cos\omega_d t\right] + \frac{f_1}{H}[2\zeta_1\omega\omega_0\sin\omega t + (\omega_0^2-\omega^2)\cos\omega t], \tag{A.4}$$

$$\bar{S}_{21}(t) = -e^{-\zeta_1\omega_0 t}\left(\frac{\zeta_1^2\omega_0^2}{\omega_d}+\omega_d\right)\sin\omega_d t, \tag{A.5}$$

$$\bar{S}_{22}(t) = -e^{-\zeta_1\omega_0 t}\left(\frac{\zeta_1\omega_0}{\omega_d}\sin\omega_d t - \cos\omega_d t\right), \tag{A.6}$$

$$\bar{S}_{23}(t) = \frac{f_1\omega e^{-\zeta_1\omega_0 t}}{H}\left[\frac{-\zeta_1\omega_0}{\omega_d}(\omega_0^2-\omega^2-2\zeta_1^2\omega_0^2-2\omega_d^2)\sin\omega_d t + (\omega_0^2-\omega^2)\cos\omega_d t\right] - \frac{f_1\omega}{H}[2\zeta_1\omega\omega_0\sin\omega t + (\omega_0^2-\omega^2)\cos\omega t], \tag{A.7}$$

$$\bar{S}_{24}(t) = \frac{f_1 e^{-\zeta_1\omega_0 t}}{H}\left\{\frac{1}{\omega_d}[\zeta_1^2\omega_0^2(\omega_0^2+\omega^2)+\omega_d^2(\omega_0^2-\omega^2)]\sin\omega_d t - 2\zeta_1\omega^2\omega_0\cos\omega_d t\right\} - \frac{f_1\omega}{H}[(\omega_0^2-\omega^2)\sin\omega t - 2\zeta_1\omega\omega_0\cos\omega t], \tag{A.8}$$

where $\omega_d = \omega_0\sqrt{1-\zeta_1^2}$, $H = (\omega_0^2-\omega^2)^2 + (2\zeta_1\omega\omega_0)^2$. Replacing $\omega_0$, $\zeta_1$ and $f_1$ in Eqs. (A.1), (A.2), …, (A.7) and (A.8) with 1, $\zeta_2$ and $f_2$ respectively, and changing $\omega_d$ and $H$ correspondingly, one obtains $\bar{S}_{31}(t)$, $\bar{S}_{32}(t)$, $\bar{S}_{33}(t)$, $\bar{S}_{34}(t)$ and $\bar{S}_{41}(t)$, $\bar{S}_{42}(t)$, $\bar{S}_{43}(t)$, $\bar{S}_{44}(t)$.

## Appendix B

$$\begin{aligned} b_0(x_{10}) = {} & r_1(x_{10})[S_{12}(S_{24}S_{33}-S_{23}S_{34})+S_{22}(S_{13}S_{34}-S_{14}S_{33})] + r_2(x_{10})S_{12}(S_{33}S_{44}-S_{34}S_{43}) \\ & + r_3(x_{10})S_{32}(S_{14}S_{23}-S_{13}S_{24}) + r_4(x_{10})[S_{32}(S_{14}S_{43}-S_{13}S_{44})+S_{42}(S_{13}S_{34}-S_{14}S_{33})] \\ & + r_1(x_{10})r_4(x_{10})[S_{22}S_{32}(S_{13}S_{44}-S_{14}S_{43})+S_{22}S_{42}(S_{14}S_{33}-S_{13}S_{34}) \\ & + S_{12}S_{32}(S_{24}S_{43}-S_{23}S_{44})+S_{12}S_{42}(S_{23}S_{34}-S_{24}S_{33})] \\ & + r_2(x_{10})r_3(x_{10})[S_{12}S_{32}(S_{23}S_{44}-S_{24}S_{43})+S_{22}S_{32}(S_{14}S_{43}-S_{13}S_{44}) \\ & + S_{42}S_{12}(S_{24}S_{33}-S_{23}S_{34})+S_{42}S_{22}(S_{13}S_{34}-S_{14}S_{33})]+S_{14}S_{33}-S_{13}S_{34}, \end{aligned} \tag{B.1}$$

$$\begin{aligned} b_{11}(x_{10}) = {} & r_2(x_{10})(S_{34}S_{43}-S_{33}S_{44})[S_{22}(S_{11}-1)-S_{12}S_{21}] \\ & + r_4(x_{10})[S_{21}S_{32}(S_{14}S_{43}-S_{13}S_{44})+S_{21}S_{42}(S_{13}S_{34}-S_{14}S_{33}) \\ & + S_{32}(S_{11}-1)(S_{23}S_{44}-S_{24}S_{43})+S_{42}(S_{11}-1)(S_{24}S_{33}-S_{23}S_{34})] \\ & + (S_{11}-1)(S_{23}S_{34}-S_{24}S_{33})-S_{21}(S_{13}S_{34}-S_{14}S_{33}), \end{aligned} \tag{B.2}$$

$$b_{12}(x_{10}) = r_2(x_{10})[S_{41}S_{12}(S_{23}S_{34} - S_{24}S_{33}) + S_{41}S_{22}(S_{14}S_{33} - S_{13}S_{34}) + S_{12}(S_{31} - 1)(S_{24}S_{43} - S_{23}S_{44}) + S_{22}(S_{31} - 1)(S_{13}S_{44} - S_{14}S_{43})] + r_4(x_{10})(S_{14}S_{23} - S_{13}S_{24})[S_{42}(S_{31} - 1) - S_{41}S_{32}] + (S_{31} - 1)(S_{13}S_{24} - S_{14}S_{23}), \quad \text{(B.3)}$$

$$b_{21}(x_{10}) = r_1(x_{10})(S_{33}S_{44} - S_{34}S_{43})[S_{22}(S_{11} - 1) - S_{12}S_{21}] + r_3(x_{10})[S_{21}S_{32}(S_{13}S_{44} - S_{14}S_{43}) + S_{32}(S_{11} - 1)(S_{24}S_{43} - S_{23}S_{44}) + S_{21}S_{42}(S_{14}S_{33} - S_{13}S_{34}) + S_{42}(S_{11} - 1)(S_{23}S_{34} - S_{24}S_{33})] + (S_{11} - 1)(S_{34}S_{43} - S_{33}S_{44}), \quad \text{(B.4)}$$

$$b_{22}(x_{10}) = r_1(x_{10})[S_{41}S_{12}(S_{24}S_{33} - S_{23}S_{34}) + S_{41}S_{22}(S_{13}S_{34} - S_{14}S_{33}) + S_{12}(S_{31} - 1)(S_{23}S_{44} - S_{24}S_{43}) + S_{22}(S_{31} - 1)(S_{14}S_{43} - S_{13}S_{44})] + r_3(x_{10})(S_{13}S_{24} - S_{14}S_{23})[S_{42}(S_{31} - 1) - S_{41}S_{32}] + (S_{31} - 1)(S_{13}S_{44} - S_{14}S_{43}) + S_{41}(S_{14}S_{33} - S_{13}S_{34}), \quad \text{(B.5)}$$

$$b_{31}(x_{10}) = r_1(x_{10})[r_4(x_{10})(S_{42}S_{34} - S_{32}S_{44}) - S_{34}][S_{22}(S_{11} - 1) - S_{12}S_{21}] + r_2(x_{10})r_3(x_{10})(S_{32}S_{44} - S_{42}S_{34})[S_{22}(S_{11} - 1) - S_{12}S_{21}] + r_3(x_{10})S_{32}[S_{24}(S_{11} - 1) - S_{21}S_{14}] + r_4(x_{10})(S_{11} - 1)(S_{32}S_{44} - S_{42}S_{34}) + S_{34}(S_{11} - 1), \quad \text{(B.6)}$$

$$b_{32}(x_{10}) = r_1(x_{10})\{[1 - r_4(x_{10})S_{42}](S_{31} - 1) + r_4(x_{10})S_{32}S_{41}\}(S_{22}S_{14} - S_{12}S_{24}) + r_2(x_{10})S_{12}[-S_{44}(S_{31} - 1) + S_{34}S_{41}] + r_2(x_{10})r_3(x_{10})(S_{12}S_{24} - S_{14}S_{22})[-S_{42}(S_{31} - 1) + S_{32}S_{41}] + r_4(x_{10})S_{14}[S_{42}(S_{31} - 1) - S_{32}S_{41}] - S_{14}(S_{31} - 1), \quad \text{(B.7)}$$

$$b_{41}(x_{10}) = r_1(x_{10})[S_{33} - r_4(x_{10})(S_{42}S_{33} - S_{32}S_{43})][S_{22}(S_{11} - 1) - S_{12}S_{21}] + r_2(x_{10})r_3(x_{10})(S_{42}S_{33} - S_{32}S_{43})[S_{22}(S_{11} - 1) - S_{12}S_{21}] + r_3(x_{10})S_{32}[-S_{23}(S_{11} - 1) + S_{21}S_{13}] + r_4(x_{10})(S_{11} - 1)(S_{42}S_{33} - S_{32}S_{43}) - S_{33}(S_{11} - 1), \quad \text{(B.8)}$$

$$b_{42}(x_{10}) = r_1(x_{10})\{[1 - r_4(x_{10})S_{42}](S_{31} - 1) + r_4(x_{10})S_{32}S_{41}\}(S_{12}S_{23} - S_{22}S_{13}) + r_2(x_{10})S_{12}[S_{43}(S_{31} - 1) - S_{33}S_{41}] + r_2(x_{10})r_3(x_{10})(S_{22}S_{13} - S_{12}S_{23})[-S_{42}(S_{31} - 1) + S_{32}S_{41}] + r_4(x_{10})S_{13}[-S_{42}(S_{31} - 1) + S_{32}S_{41}] + S_{13}(S_{31} - 1). \quad \text{(B.9)}$$

## Appendix C

$$J_0 = (a_{11}a_{22} - a_{21}a_{12})(a_{33}a_{44} - a_{34}a_{43}) - (a_{11}a_{32} - a_{31}a_{12})(a_{23}a_{44} - a_{24}a_{43}) - (a_{11}a_{42} - a_{41}a_{12})(a_{24}a_{33} - a_{23}a_{34}) - (a_{13}a_{44} - a_{14}a_{43})(a_{31}a_{22} - a_{21}a_{32}) - (a_{14}a_{33} - a_{13}a_{34})(a_{41}a_{22} - a_{21}a_{42}) + (a_{14}a_{23} - a_{13}a_{24})(a_{41}a_{32} - a_{31}a_{42}), \quad \text{(C.1)}$$

$$J_1 = -a_{11}(a_{22}a_{33} - a_{23}a_{32} + a_{22}a_{44} - a_{24}a_{42} + a_{33}a_{44} - a_{34}a_{43}) - a_{22}(a_{33}a_{44} - a_{34}a_{43}) + a_{12}(a_{21}a_{33} - a_{31}a_{23} + a_{21}a_{44} - a_{41}a_{24}) - a_{13}(a_{21}a_{32} - a_{31}a_{22} + a_{41}a_{34} - a_{31}a_{44}) + a_{14}(a_{41}a_{33} - a_{31}a_{43} + a_{41}a_{22} - a_{21}a_{42}) + a_{32}(a_{23}a_{44} - a_{24}a_{43}) + a_{42}(a_{24}a_{33} - a_{23}a_{34}), \quad (C.2)$$

$$J_2 = a_{11}a_{22} - a_{12}a_{21} + a_{11}a_{33} - a_{13}a_{31} + a_{11}a_{44} - a_{14}a_{41} + a_{22}a_{33} - a_{23}a_{32} + a_{22}a_{44} - a_{24}a_{42} + a_{33}a_{44} - a_{34}a_{43}, \quad (C.3)$$

$$J_3 = -(a_{11} + a_{22} + a_{33} + a_{44}). \quad (C.4)$$

## References


[1] S.W. Shaw, P.J. Homes, A periodically forced piecewise linear oscillator, *Journal of Sound and Vibration* 90 (1983) 129–155.

[2] D.P. Jin, H.Y. Hu, Vibro-impacts and their typical behaviors of mechanical systems, *Advances in Mechanics* 29 (1999) 155–164 (in Chinese).

[3] M.L. Lv, The impact theory and the variational mass dynamics, in: Q.H. Du (Editor-in-chief), *A Handbook of Engineering Mechanics*, Higher Education Press, Beijing, 1992 (in Chinese).

[4] S.W. Shaw, The dynamics of a harmonically excited system having rigid amplitude constraints, *Transactions of the American Society of Mechanical Engineers, Journal of Applied Mechanics* 52 (1985) 453–464.

[5] C. Gontier, C. Toulemonde, Approach to the periodic and chaotic behavior of the impact oscillator by a continuation method, *Europe Journal of Mechanics, A/Solids* 16 (1997) 141–163.

[6] G.S. Whiston, Global dynamics of a vibro-impacting linear oscillator, *Journal of Sound and Vibration* 118 (1987) 395–424.

[7] S. Foale, S.R. Bishop, Bifurcations in impact oscillations, *Nonlinear Dynamics* 6 (1994) 285–299.

[8] H.Y. Hu, Simulation complexities in the dynamics of a continuously piecewise-linear oscillator, *Chaos, Solitons and Fractals* 5 (1995) 2201–2212.

[9] H.Y. Hu, Primary resonance of a harmonically forced oscillator with a pair of symmetric set-up elastic stops, *Journal of Sound and Vibration* 207 (1997) 393–401.

[10] S.R. Bishop, M.G. Thompson, S. Foale, Prediction of period-1 impacts in a driven beam, *Proceedings of the Royal Society of London, Series A* 452 (1996) 2579–2592.

[11] A.P. Ivanov, Impact oscillations, linear theory of stability and bifurcation, *Journal of Sound and Vibration* 178 (1994) 361–378.

[12] C. Toulemonde, C. Gontier, Multiple degree of freedom impact oscillator, *Europe Journal of Mechanics, A/Solids* 16 (1997) 879–904.

[13] C. Toulemonde, C. Gontier, Sticking motions of impact oscillator, *Europe Journal of Mechanics, A/Solids* 18 (1998) 339–366.

[14] G.W. Luo, J.H. Xie, Bifurcations and chaos in a system with impacts, *Physica D* 148 (2001) 183–200.

[15] G.W. Luo, J.H. Xie, S.H.L. Guo, Periodic motions and global bifurcations of a two degree-of-freedom system with plastic vibro-impact, *Journal of Sound and Vibration* 240 (2001) 837–858.

[16] S.A. Kember, V.I. Babitsky, Excitation of vibro-impact systems by periodic impulses, *Journal of Sound and Vibration* 227 (1999) 427–447.

[17] D.P. Jin, H.Y. Hu, Periodic impacting motions and their stability of a dual component system, *Acta Mechanica Sinica* 13 (1997) 366–376.

[18] Q.H. Li, Q.S. Lu, Analysis to motions of a two-degree-of-freedom vibro-impact system, *Acta Mechanica Sinica* 33 (2001) 776–786 (in Chinese).

[19] V.I. Babitsky, *Theory of Vibro-Impact Systems and Applications*, Springer, Berlin, 1998.

[20] M.L. Lv, Note on the coefficient of friction during an oblique collision, *Acta Mechanica Solida Sinica* 3 (1987) 282–284 (in Chinese).
[21] S.B. Ratner, E.E. Styller, Characteristics of impact friction and wear of polymeric materials, *Wear* 73 (1981) 213–234.
[22] R.M. Brach, Rigid body collisions, *Transactions of the American Society of Mechanical Engineers, Journal of Applied Mechanics* 56 (1989) 133–138.
[23] W.J. Stronge, Rigid body collisions with friction, *Proceedings of the Royal Society of London, Series A* 431 (1990) 169–181.
[24] W.J. Stronge, Friction in collisions; resolution of a paradox, *Journal of Applied Physics* 69 (1991) 610–612.
[25] W.J. Stronge, Swerve during three-dimensional impact of rough rigid bodies, *Transactions of the American Society of Mechanical Engineers, Journal of Applied Mechanics* 61 (1994) 605–611.
[26] Y. Wang, M.T. Mason, Two-dimensional rigid-body collisions with friction, *Transactions of the American Society of Mechanical Engineers, Journal of Applied Mechanics* 59 (1992) 635–642.
[27] A.D. Lewis, R.J. Rogers, Experimental and numerical study of forces during oblique impact, *Journal of Sound and Vibration* 125 (1988) 403–412.
[28] C.T. Lim, W.J. Stronge, Oblique elastic–plastic impact between rough cylinders in plane strain, *International Journal of Engineering Science* 37 (1999) 97–122.
[29] F. Génot, B. Brogliato, New results on Painlevé paradoxes, *Europe Journal of Mechanics, A/Solids* 18 (1999) 653–677.
[30] W. Han, Dynamics of Oblique-impact Vibrating Systems, Ph.D. Dissertation, Nanjing University of Aeronautics and Astronautics, Nanjing, China, 2003 (in Chinese).